Lagrangian Properties of Particles in Turbulence

Federico Toschi[1] and Eberhard Bodenschatz[2]

[1]Istituto per le Applicazioni del Calcolo, CNR, I-00161 Rome, Italy; INFN, Sezione di Ferrara, I-44100 Ferrara, Italy; Department of Physics and Department of Mathematics and Computer Science, Eindhoven University of Technology, 5600 MB Eindhoven, The Netherlands; and International Collaboration for Turbulence Research; email: toschi@iac.cnr.it

[2]Max Planck Institute for Dynamics and Self-Organization, D-37077 Goettingen, Germany; Laboratory of Atomic and Solid-State Physics and Sibley School of Mechanical and Aerospace Engineering, Cornell University, Ithaca, New York 14853; Institute for Nonlinear Dynamics, University of Goettingen, D-37073 Goettingen, Germany; and International Collaboration for Turbulence Research

Annu. Rev. Fluid Mech. 2009. 41:375–404

First published online as a Review in Advance on September 25, 2008

The *Annual Review of Fluid Mechanics* is online at fluid.annualreviews.org

This article's doi:
10.1146/annurev.fluid.010908.165210

0066-4189/09/0115-0375$20.00

Key Words

anomalous scaling, mixing, dispersion, particle tracking, intermittency

Abstract

The Lagrangian description of turbulence is characterized by a unique conceptual simplicity and by an immediate connection with the physics of dispersion and mixing. In this article, we report some motivations behind the Lagrangian description of turbulence and focus on the statistical properties of particles when advected by fully developed turbulent flows. By means of a detailed comparison between experimental and numerical results, we review the physics of particle acceleration, Lagrangian velocity structure functions, and pairs and shapes evolution. Recent results for nonideal particles are discussed, providing an outlook on future directions.

1. INTRODUCTION AND FUNDAMENTALS

The flow of a strongly stirred viscous fluid is turbulent, and its spatiotemporal dynamics is characterized by a large number of dynamically active and interacting degrees of freedom (e.g., see Frisch 1995, Monin & Yaglom 1975, Nelkin 2000, Pope 2000, Tennekes & Lumley 1972, and references therein). One can describe the properties of turbulence in terms of variables defined at points fixed in space (i.e., the Eulerian reference frame) or the reference frame of individual fluid particles carried by the flow (e.g., see Yeung 2002, and references therein). The latter Lagrangian description captures the temporal evolution of a turbulent flow, as it is not affected by large-scale turbulence sweeping (see L'vov et al. 1997). As Taylor (1921) recognized early on in his seminal work on turbulent diffusion, transport issues are addressed naturally from the Lagrangian viewpoint, which has since been successfully employed in the theoretical treatment of turbulent mixing (Sawford 2001, Shraiman & Siggia 2000, Yeung 2002). Lagrangian stochastic models are widely used to model processes ranging from atmospheric pollution transport to turbulent combustion (see Lamorgese et al. 2007, Pope 2000, Weil et al. 1992). Lagrangian concepts are useful when considering entrainment processes at turbulent/laminar interfaces (see Holzner et al. 2008, and references therein). There are also many applications in which the transport or aggregation of particulates in turbulence is important. One important example is related to atmospheric physics and is concerned with droplet formation in wet clouds. There the intermittent properties of turbulent particle acceleration combined with the inertial effects of small condensed droplets are thought to lead to increased droplet collisions and the formation of larger droplets (see Falkovich et al. 2002, Kostinski & Shaw 2005). Turbulence also plays a major role in determining the radiative emissivity of clouds. The parameterization of turbulence-cloud interactions is currently a large uncertainty in climate forecast simulations. For further details, we refer the reader to recent reviews by Shaw (2003) and Warhaft (2008). **Figure 1** shows the evolution of tracers in a turbulent flow.

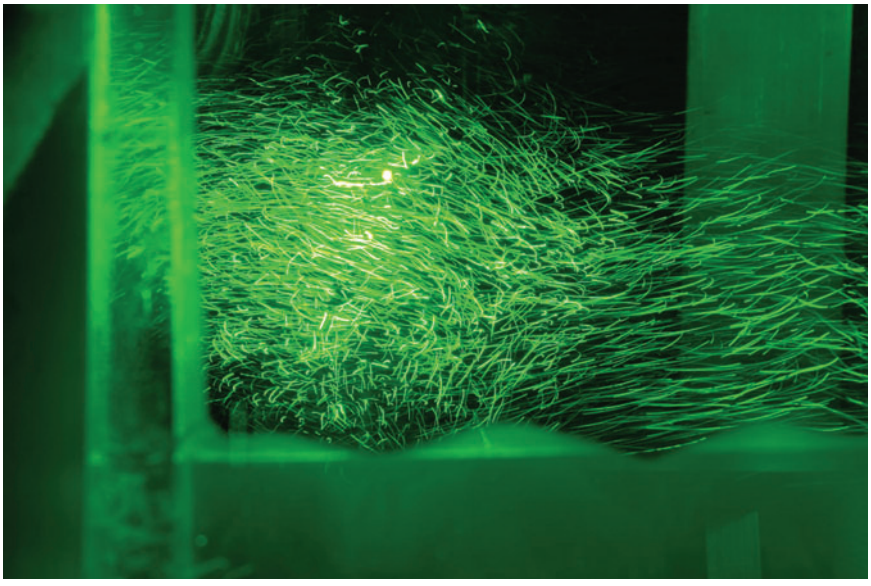

Figure 1

Polystyrene spheres 25 μm in diameter are used as tracers in experiments and illuminated by a green YAG laser with a mean output power as high as 35 W. Photo courtesy of E. Bodenschatz.

The Lagrangian description of turbulence has begun to advance our knowledge significantly. Example applications include analytical approaches to tackling the statistical properties of homogeneous and isotropic turbulence as a field theory (Lagrangian history direct interaction; see Kraichnan 1966); the connection between turbulence intermittency and statistically preserved structures (Castiglione & Pumir 2001, Celani & Vergassola 2001, Falkovich et al. 2001); models for the evolution of Lagrangian clusters, also known as the statistical geometry of turbulence (Chertkov et al. 1999; Pumir et al. 2000, 2001); the Lagrangian evolution of material lines, vorticity, and strain (Guala et al. 2005, Lüthi et al. 2005); Lagrangian tools used to improve subgrid-scale modeling in large eddy simulation (Bou-Zeid et al. 2005, Meneveau et al. 1996, Pope 2004); stochastic models to regularize velocity gradients in turbulence (Chevillard & Meneveau 2006); studies of the singularities of the Euler equation (Constantin 2001); and computational methods to numerically integrate Eulerian flows (Monaghan 1988).

Yeung (2002) reviewed the Lagrangian properties of turbulence, focusing mainly on computational aspects: At that time, experimental measurements at high Reynolds numbers were limited to single-particle statistics. Present experiments are capable of following hundreds of particles at very high Reynolds numbers (e.g., see Xu et al. 2008), and numerical capabilities are increasing at a rapid pace.

Owing to the vast amount of work and literature on Lagrangian turbulence, we limit our discussion to tracer and particle dynamics. Furthermore, we focus almost exclusively on those studies in which major efforts in comparing experimental and numerical results have been made. A side-by-side comparison of results from experiment, numerics, and theory is presented whenever possible. We note that we do not cover several important aspects of the Lagrangian properties of turbulence, including relative dispersion (Salazar & Collins 2009), the study of velocity gradients (Gulitski et al. 2007a), and Lagrangian stochastic models (Sawford 2001). The review is organized as follows: Section 2 details the experimental and numerical methods, Section 3 reviews results on neutral tracers, and Section 4 presents an outlook on future directions.

The dynamics of an incompressible turbulent fluid is described by the Navier-Stokes equation along with the incompressibility condition $\nabla \cdot \boldsymbol{u} = 0$. In terms of the fluid particle acceleration $\boldsymbol{a}$, the Navier-Stokes equation reads

$$\boldsymbol{a} = \frac{\partial \boldsymbol{u}}{\partial t} + (\boldsymbol{u} \cdot \nabla)\boldsymbol{u} = -\frac{\nabla p}{\rho} + \frac{1}{Re}\nabla^2 \boldsymbol{u}, \tag{1}$$

where p is the pressure, ρ is the fluid density, $Re = Lu'/\nu$ is the Reynolds number, u' is the root-mean-squared velocity, and ν is the kinematic viscosity. By means of Kolmogorov's (1941) phenomenology, the largest (spatial and temporal) scales are given by the energy-injection length scales L and eddy turnover time T_L, whereas the smallest scales are given by the Kolmogorov length $\eta = (\nu^3/\varepsilon)^{1/4}$ and the Kolmogorov time $\tau_\eta = (\nu/\varepsilon)^{1/2}$, where $\varepsilon = \nu \sum_{ij} (\partial_i u_j + \partial_j u_i)^2$ is the energy-dissipation rate. The scale separation in a turbulent flow is thus $L/\eta = Re^{3/4}$ and $T_L/\tau_\eta = Re^{1/2} \propto R_\lambda$ (where R_λ is the Taylor microscale Reynolds number[1]). Between these scales is the so-called inertial range of turbulence. The Eulerian inertial range increases with Reynolds number by a factor $Re^{1/4}$ faster than the Lagrangian inertial range. Therefore, to observe inertial-range scaling in the Lagrangian framework, even larger Reynolds numbers are necessary. In nature, flows can attain Reynolds numbers on the order of 10^7 or more, and the scale separation can be very large. For a large scaling range, the universal properties of turbulence should become apparent,

[1] R_λ is the Reynolds number, $R_\lambda = u'\lambda/\nu$, defined in terms of the Taylor scale, $\lambda = u'/\langle(\partial u/\partial x)^2\rangle^{1/2}$, and u' is the root-mean-squared velocity. For isotropic and homogeneous flows, R_λ is related to Re by $R_\lambda = \sqrt{15\,Re}$.

and they are expected to be independent of the energy-injection mechanism at the largest scales. This requirement increases the demands on both simulations and experiments.

Researchers study the Lagrangian properties of a turbulent flow from the viewpoint of fluid particles (which we refer to as tracers below). The tracers' trajectories can be either directly measured or calculated from their Lagrangian velocity $\boldsymbol{v}(t)$ given by Equation 1 by integrating

$$\boldsymbol{v}(t) = \frac{d\boldsymbol{x}(t)}{dt} = \boldsymbol{u}[\boldsymbol{x}(t); t]. \tag{2}$$

Below we discuss the Lagrangian dynamics of particles that have a different density ρ_p than the fluid ρ_f. As long as the diameter d of the particles is small compared to the Kolmogorov length η, the finite volume of the particle makes the integration of a different set of equations of motion (e.g., Equation 3) necessary. A commonly used, simplified, but nontrivial modeling for passively advected particles (sufficiently dilute to neglect collisions) is the following (see Auton et al. 1988, Babiano et al. 2000, Gatignol 1983, Maxey & Riley 1983):

$$\frac{d}{dt}\boldsymbol{x}(t) = \boldsymbol{v}(t), \quad \frac{d}{dt}\boldsymbol{v}(t) = \beta\frac{D}{Dt}\boldsymbol{u}[\boldsymbol{x}(t); t] - \frac{1}{\tau}\{\boldsymbol{v}(t) - \boldsymbol{u}\}, \tag{3}$$

where gravity and lift forces have been neglected. Owing to their inertia, measured by the Stokes time $\tau = a^2/(3\beta\nu)$ [where a is the particle radius, ν is the fluid viscosity, and $\beta = 3\rho_f/(2\rho_p + \rho_f)$], such particles depart from fluid streamlines and distribute nonhomogeneously (see Balkovsky et al. 2001, Crisanti et al. 1992, Maxey 1987).

2. METHODS

New experimental techniques, along with ever-improving computational capabilities, enable systematic and quantitative investigations of Lagrangian turbulence at moderate to high Reynolds numbers. The major difficulty lies in resolving accurately, in space and in time, the trajectories of particles. For direct numerical simulations (DNS) of the Navier-Stokes equations, the numerical costs limit the achievable Reynolds numbers. For DNS in a periodic box, the largest simulations that resolve a few T_L in time have seen an increase, from 1970 to 2007, of the maximal attainable values of R_λ from $\approx$50 to $\approx$1000 (see **Figure 2*b***). In experiments, the observational volume and acquisition time must be of the order of the size L^3 and turnover time T_L of the largest eddies in the flow, respectively, to measure Lagrangian information over all scales. In addition, the temporal resolution must be much better than the Kolmogorov scales (Voth et al. 2001). **Figure 2*a*** shows the Kolmogorov times for different flows and different fluids.

2.1. Computational Techniques

Computational investigations of the Lagrangian properties of turbulence numerically solve the Navier-Stokes equation (Equation 1) and use the Eulerian velocity field $\boldsymbol{u}(\boldsymbol{x}, t)$ to evolve the trajectories of tracers $\boldsymbol{x}(t)$, integrating Equation 2, or, for particles with inertia, integrating more complicated equations such as Equation 3. Numerical investigations of the Lagrangian properties of turbulence are computationally more demanding than those of the Eulerian velocity alone (Riley & Patterson 1974). Commonly used techniques involve standard pseudospectral methods for the Eulerian field with dealiasing (Yeung 2002). The continuous advancement in computational capabilities, whose direct implication for fluid dynamics turbulence has been recently reviewed by Celani (2007), allows the attainment of Reynolds numbers up to the order of $R_\lambda \sim 1000$ (Ishihara et al. 2007). Computationally, it is easy to access multitime, multiparticle correlations; the major

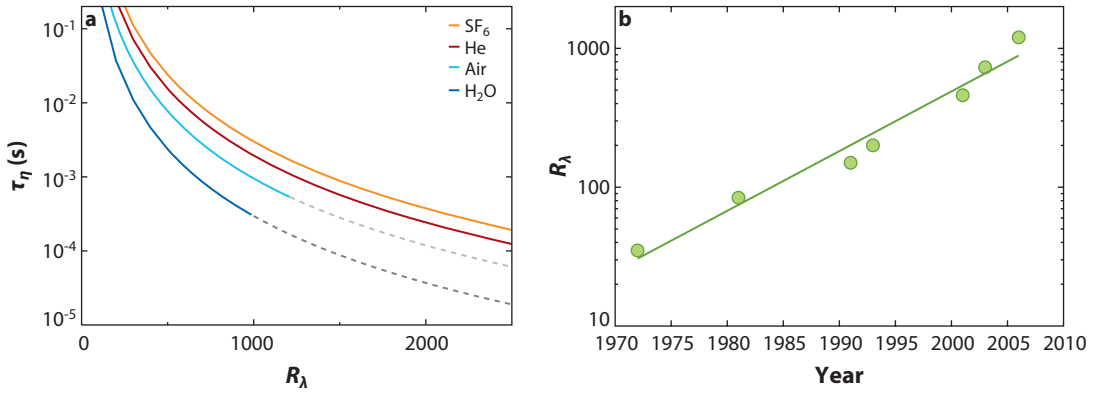

Figure 2

(*a*) Kolmogorov time τ_η versus microscale Reynolds number R_λ in highly turbulent flows suitable for Lagrangian measurements. The water data are from the experiment by La Porta et al. (2001) and Voth et al. (2002) (energy-injection scale $L = 0.07$ m, $R_\lambda < 1000$), air data are from the experiment by Mydlarski & Warhaft (1998) ($L = 0.5$ m, $R_\lambda < 1200$), low-temperature helium data are from experiments by Tabeling et al. (1996) ($L = 0.02$ m, $R_\lambda < 3000$), and room-temperature compressed SF_6 is estimated ($L = 0.07$ m, $R_\lambda < 3500$, $p = 20$ bar). Gray dashed lines indicate Reynolds numbers outside the limits of the current existing facilities. (*b*) The trend of R_λ versus year for state-of-the-art numerical simulations. Data are from Celani 2007, table 1.

limiting factor, owing to statistical requirements, is the necessity of creating huge databases that can be time-consuming to access. As a consequence, high-resolution computations often suffer from the limited number of large-scale eddy turnover times, which in turn may leave residual anisotropy on the largest scales (even with perfectly isotropic forcing schemes). The recent quest for the highest Reynolds number flow seems to conflict with accuracy requirements. When looking at small-scale quantities (which are particularly intermittent, such as the acceleration), a better resolved simulation (i.e., larger $k_{max} \cdot \eta$, where k_{max} is the largest resolved wave number in the simulation) at a lower resolution (i.e., with a smaller number of collocation points) can be more accurate than a higher-resolution simulation with poorer accuracy at small scales (see Ishihara et al. 2007, Schumacher 2007).

The numerical schemes in use today have been well tested; as for the interpolation schemes, their accuracy and impact on statistical quantities have been the subject of several investigations (Balachandar & Maxey 1989, Homann et al. 2007a, Rovelstad et al. 1994, Yeung & Pope 1988).

In recent years, much progress has been made in developing schemes capable of numerically integrating the dynamics of finite-size and inertial particles. Examples include simulations of air bubbles in water using front-tracking techniques (e.g., see Unverdi & Tryggvason 1992), simulations of solid finite-size particles using the lattice Boltzmann method (Cate et al. 2004), and simulations using the Physalis method (Perrin & Hu 2006, Zhang & Prosperetti 2005) or resolving the full fluid dynamical interaction between the particle and the fluid (Burton & Eaton 2005).

These methods will most likely become standard tools in the future, but presently, because of their higher numerical costs, they do not allow the simulation of the large number of particle tracks needed for converged statistics. Therefore, most studies of the Lagrangian properties of turbulence trace point-like particles. Although this poses no problems for passive tracers, some level of modeling is necessary for particles; consequently, a validation of the models against experiments is mandatory.

2.2. Experimental Techniques

The experimental investigation of turbulent flows can be separated into Eulerian and Lagrangian techniques. Here we summarize and discuss both of them, pointing out challenges for Lagrangian measurements.

2.2.1. Eulerian measurements. The investigation of turbulent flows has been dominated by Eulerian measurements (i.e., measurements at fixed location in the flow), in which the mean velocities are larger than those of the turbulent fluctuations. The most suitable measurement techniques are miniature hot wires that can be used to measure the temporal evolution of the velocity field at several locations. The technique is intrusive as the sensor is held upstream into the flow. By invoking Taylor's frozen-flow hypothesis, it is then possible to transform the data from the temporal to the spatial domain. Although these measurements are fully Eulerian, they can be employed to calculate some quantities (e.g., fluid particle acceleration) that are more easily determined from Lagrangian measurements. By using the relations between the fourth-order velocity structure functions and pressure structure functions, Gylfason et al. (2004), Hill & Wilczak (1995), and Monin & Yaglom (1975) were able to derive pressure and acceleration statistics for Taylor-Reynolds numbers $R_\lambda < 900$. Recently Gulitski et al. (2007b) used a sophisticated multi-hot-wire measurement technique to calculate, without invoking Taylor's frozen-flow hypothesis, spatial and temporal velocity gradients in an atmospheric boundary-layer flow at Taylor-Reynolds numbers $R_\lambda < 10{,}000$. In principle, it should have been possible to calculate the acceleration from the convective derivative of the velocity. However, the two terms almost cancel each other (Gulitski et al. 2007b), producing large uncertainties. In measuring the acceleration, Gulitski et al. (2007b) had to resort to the same analysis as Gylfason et al. (2004).

Other techniques include laser Doppler anemometry and particle-imaging velocimetry. Laser Doppler anemometry allows only point-wise measurements of velocity and thus has only limited utility. Particle-imaging velocimetry in principle allows measurements of the velocity field, but its applicability to high–Reynolds number flows is limited owing to camera resolution. It has been employed, for example, to measure local gradients at $R_\lambda < 54$ (Zeff et al. 2003).

2.2.2. Lagrangian particle tracking. Investigators use several techniques to measure the Lagrangian properties of turbulence. One early technique employed Taylor's (1921) theory of turbulent dispersion to determine the Lagrangian velocity correlation function from the scalar dispersion. Shlien & Corrsin (1974) provided a summary of measurements performed using this technique before offering a set of measurements. Another technique, pioneered by Miles et al. (1991), allows the measurement of the short-time displacements and distortions of very thin tagged lines written into the flow by a laser and then interrogated by laser-induced fluorescence. This technique, now known as molecular flow tagging velocimetry, uses no tracers (Elenbaas 2005). Because of dispersive spreading in the direction of the line, molecular flow tagging velocimetry allows tracking for limited time intervals only. By using nonlinear optical processes (multiphoton processes), it may become possible to write points into the fluid, thus reducing this complication (W. van de Water, private communication).

Presently, the most successful technique for the investigation of Lagrangian turbulence is the optical tracking of tracer particles. The technique is known as particle-tracking velocimetry, when velocities are concerned, or Lagrangian particle tracking, when position and acceleration are also determined. Particles can be passive tracers that approximate the Lagrangian motion of fluid elements, have inertia, or have a size larger than the smallest scales of the flow. Snyder & Lumley (1971) provided the first systematic set of particle-tracking velocity measurements from

wind-tunnel grid turbulence, whereas Sato & Yamamoto (1987) have reported similar measurements in water-tunnel grid turbulence. Three-dimensional Lagrangian particle tracking using multiple cameras for the stereoscopic reconstruction of particle tracks was pioneered by Virant & Dracos (1997) and further developed by Ott & Mann (2000). The first measurements at high Reynolds numbers using direct optical imaging were accomplished by means of silicon-strip-detector technology derived from high-energy physics experiments (Mordant et al. 2004a,b; La Porta et al. 2001; Voth et al. 2001, 2002); however, only single-particle dynamics could be investigated. Today the technology of complementary metal-oxide semiconductor cameras allows the tracking of many particles at rates equivalent to those of the silicon strip detectors, but with only one-quarter of the spatial resolution (Bourgoin et al. 2006). Recently, improved three-dimensional particle-tracking velocimetry techniques allow access to velocity gradients along particle trajectories (Lüthi et al. 2005). The same technique has been extended to scanning particle-tracking velocimetry to reach even larger particle densities (Hoyer et al. 2005). Alternative techniques to direct imaging include digital holographic measurements (e.g., see Salazar et al. 2008, and references therein).

Another technique currently in use is acoustic Doppler (Mordant et al. 2001, 2002, 2004c; Qureshi et al. 2007), in which the measurements are limited to particles approximately five times larger than the Kolmogorov scale. The same technique has now been applied to extended laser Doppler measurements (Volk et al. 2008b), in which small passive tracers are possible. Laser Doppler techniques have also been used to measure acceleration (Lehmann et al. 2002, Volk et al. 2008b). It is important to note that this technique does not give position resolution and only allows the tracking of a single particle.

A recent development involves instrumented particles that are promising tools to explore Lagrangian turbulence (Gasteuil et al. 2007, Shew et al. 2007). These particles can include sensors capable of measuring local quantities such as temperature or acceleration and transmitting the signal in real time to receiving stations. The current large size of the particles limits their utility for turbulent flows, but further miniaturization of the electronics and the power source shows promising results.

Lagrangian measurements remain challenging for high–Reynolds number turbulent flows. To measure meaningful Lagrangian information over all scales, the interrogation volume and acquisition time must be of the order of the size L^3 and turnover time T_L of the largest eddies in the flow. In addition, the spatial and temporal resolution of the detection process must be better than the characteristic distance and timescales of the smallest eddies, defined by the Kolmogorov length η and the Kolmogorov time τ_η. For homogeneous isotropic turbulence, the Kolmogorov scales are related to the microscale Reynolds number R_λ, the largest scale of the flow L, and the kinematic viscosity ν according to $\tau_\eta = (15^{3/2}L^2)/(R_\lambda^3\nu)$ and $\eta = (15^{3/4}L)/(R_\lambda^{3/2})$. From these relations, we can see that experimentally resolvable scales at high R_λ require large L and small ν.

The best combination of current Lagrangian measurement technologies is limited to observation volumes of ≈10 cm and timescales slower than 10^{-5} s. Therefore, highly turbulent flows, in which one can hope to investigate the full Lagrangian field over all scales, are best studied in the laboratory. Atmospheric flows with $L \approx 100$ m, $\eta \approx 0.5$ mm, and $\tau_\eta \approx 0.04$ s (Kurien et al. 2000) are beyond the capabilities of current technologies. Instrumented particles are promising (Shew et al. 2007), if they can be miniaturized to a 1-mm diameter, while being kept approximately neutrally buoyant.

High–Reynolds number laboratory flows of $R_\lambda > 1000$ for Lagrangian investigations are best generated using fluids with relatively low kinematic viscosity, such as water (Voth et al. 1998), compressed gases (such as SF_6 at 20 bar), and low-temperature helium gas (Tabeling et al. 1996). In these cases, it is possible to build closed-flow, table-top turbulence generators with turbulent

velocity fluctuations, which are large compared with the mean flow rate and thus are ideally suited for Lagrangian particle-tracking experiments. In the case of helium gas, microscale Reynolds numbers up to $R_\lambda \approx 3000$ have been achieved (Tabeling et al. 1996), and hydrogen snow can be used as a tracer (Bewley et al. 2006). In addition to flows with negligible mean flow, high Reynolds numbers can be generated in active-grid wind tunnels. In this case, to keep a particle in view for a sufficient time, one must move the measurement system with the mean flow (Ayyalasomayajula et al. 2006).

Figure 2*a* shows τ_η as a function of R_λ for different fluids and laboratory flows. The time resolution of current measurement systems is sufficient to resolve up to $\tau_\eta \approx 10^{-4}$ s. Voth et al. (2002) have demonstrated that a temporal oversampling of 10 to 100 times τ_η is necessary to measure acceleration. This limits the attainable R_λ in current flows to ≈1000. The only possibility of overcoming this limitation is to increase the largest scales L while keeping the kinematic viscosity ν small. Such a flow system has been established at the Max Planck Institute for Dynamics and Self-Organization in Goettingen. In this system, a total of 11 tons of SF_6 is available to pressurize two large pressure vessels to 15 bar. One of the pressure vessels is a turbulence tunnel with active grids, in which sleds allow optical particle tracking up to $R_\lambda \approx 10{,}000$. The other pressure vessel can house closed-flow, table-top turbulence generators, with $R_\lambda \approx 4000$ achievable at measurable scales.

3. THE LAGRANGIAN DYNAMICS OF TURBULENCE

One of the most intriguing features of Lagrangian turbulence involves the strong acceleration events associated with small-scale vortical motions. One can quite easily attain acceleration events in excess of 1500 times the acceleration of gravity in turbulent flows (La Porta et al. 2001). These high-acceleration events may possibly explain the reluctance of mosquitoes to fly when moderate winds are present (La Porta et al. 2001).

Velocity differences along Lagrangian trajectories also become more intermittent the smaller the time increment becomes (Mordant et al. 2002, 2004c). Velocity increments at small time gaps are closely related to acceleration.

Figure 3 shows a vis-à-vis comparison of a high-acceleration event from experiment and from DNS. The presence of small-scale vorticity in turbulence has long been studied (Douady et al. 1991, Moisy & Jiménez 2004, La Porta et al. 2000, She et al. 1991, Siggia 1981, Vincent & Meneguzzi 1991); however, it came as a surprise that Lagrangian tracers can persist in a small-scale vortex for a time exceeding the local eddy turnover time (i.e., $10–15\tau_\eta$) (Biferale et al. 2005c, Toschi et al. 2005), and while acceleration is intermittent, its most intense fluctuations can be associated with motions in small-scale vortical structures (Biferale et al. 2005c, Mordant et al. 2004c, La Porta et al. 2000, Voth et al. 2001).

The acceleration magnitude remains correlated for a long time (Mordant et al. 2002, 2004b,c; Toschi et al. 2005; Yeung & Pope 1989), and these long correlations are associated with tracers trapped in small-scale vortices (Biferale et al. 2005c, Mordant et al. 2004c, Toschi et al. 2005). Consequently, acceleration cannot be modeled as a simple random noise: At least a two-times model is necessary (Mordant et al. 2002).

Using DNS, Biferale et al. (2005c) observed that the trapping of fluid particles in vortical structures also has a strong signature on the statistics of Lagrangian velocity structure functions (LVSFs). The presence of these vortical motions triggered multiple studies aimed at understanding their statistics in relation to the geometrical properties of trajectories. By correlating the acceleration with the local velocity or vorticity fields, Biferale & Toschi (2005), Mordant et al. (2004c), and Toschi et al. (2005) studied the statistics of high-acceleration events associated with strong vortical motion (using slightly different measures, including centripetal, longitudinal accelerations, and

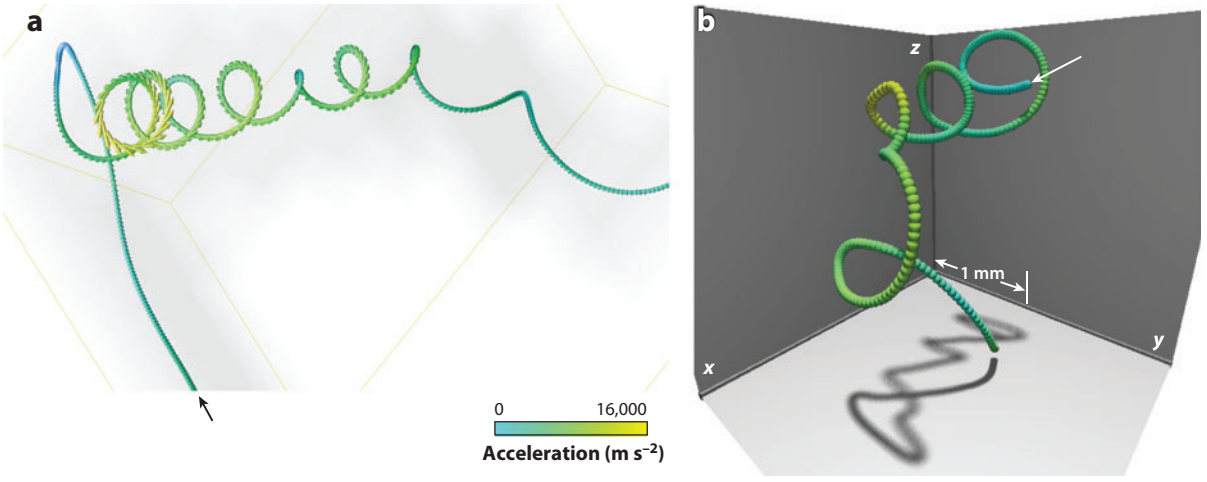

Figure 3

(*a*) A trajectory of a fluid tracer in a small-scale vortex filament in a turbulent flow from a numerical simulation at $R_\lambda \sim 280$. Colors and arrows indicate the magnitude and direction of the velocity (see Biferale et al. 2004a, Toschi et al. 2005). (*b*) Trajectory of a high-acceleration event of a 46-μm-diameter tracer particle in turbulence at $R_\lambda = 970$ recorded at a frame rate of 70,000 frames per second. The position of the particle at each of the 278 frames is represented by a sphere. The colors represent the acceleration magnitude, as indicated by the scale. Figure reproduced from Voth et al., "Measurement of particle accelerations in fully developed turbulence," *J. Fluid Mech.*, 469:121–60, 2002, with permission of Cambridge University Press.

variations thereof). When accelerations are averaged over a sliding window of $\sim 10\tau_\eta$, the accelerations (Toschi et al. 2005) and the joint acceleration-enstrophy probability distribution functions (PDFs) (Biferale et al. 2006) are unchanged for centripetal accelerations, whereas these quantities are changed when using longitudinal accelerations. This suggests a simple, but effective, way to highlight the strong correlations between the observed tails in the acceleration distribution and the presence of vortical structures in the Eulerian field. Braun et al. (2006) investigated the curvature of Lagrangian trajectories, which is tightly linked to fluid particle accelerations. Xu et al. (2007a) measured experimentally curvature statistics of trajectories' paths and compared them with Braun et al.'s (2006) DNS results. Xu et al. (2007a) found that the filtered curvature is correlated with vorticity and could be used as an indicator for structures in turbulence.

In the following section we restrict our discussion to the dynamics of fluid particles that are approximated in experiments by small neutrally buoyant tracers. We review results on tracer acceleration, the statistics of Lagrangian velocity differences, and LVSFs. We also present a cursory review on the multifractal (MF) model as a possible analytical framework and some of its recent tests in the context of Lagrangian turbulence. In the MF model, there is no concept of space and vortex filaments, but remarkably, it can reproduce the observed phenomenology of Lagrangian tracers. This finding seems to imply that what really is essential are only the statistical properties of vortex filaments that a model like the MF is able to reproduce.

3.1. Acceleration

The first experimental measurements of acceleration in highly turbulent flows used detector technology modified from the CLEO III high-energy physics experiment (i.e., silicon strip detectors) (Mordant et al. 2004a, La Porta et al. 2001, Voth et al. 2001). The quality of the data from that experiment is still unsurpassed (see **Figure 4*a***).

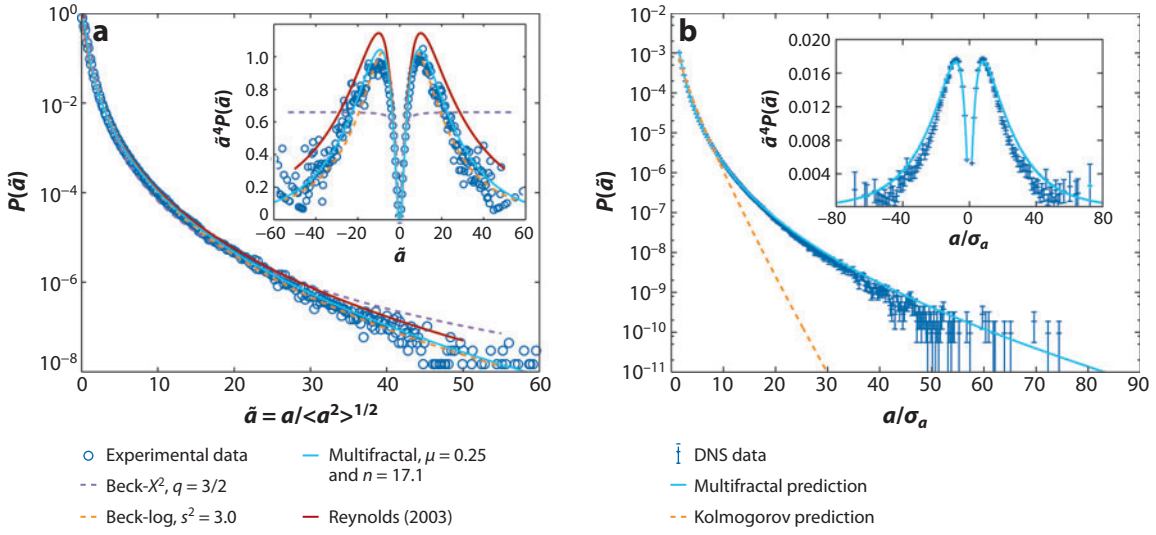

Figure 4

(*a*) Lin-log plot, comparing the experimental acceleration probability distribution function (PDF) with different models (Mordant et al. 2004a). Blue circles represent experimental data; the purple dashed line denotes Beck-χ^2, $q = 3/2$ (Beck 2001); the orange dashed line is the Beck-log, $s^2 = 3.0$ (Beck 2003); the light blue line represents the multifractal model, $\mu = 0.25$ and $n = 17.1$ (Arimitsu & Arimitsu 2004); and the red line is from Reynolds (2003). (*Inset*) Linear plot of $\tilde{a}^4 P(\tilde{a})$ versus $\tilde{a} = a/a_{rms}$. Panel *a* courtesy of Haitao Xu. (*b*) Lin-log plot of the acceleration PDF. The crosses represent the direct numerical simulation (DNS) data, the solid line is the multifractal prediction, and the dashed line is a prediction based on Kolmogorov's (1941) theory. The DNS statistics were calculated along the trajectories of 2 million particles, 3.6×10^9 events in total. The statistical uncertainty in the PDF was quantified by assuming that fluctuations grow similar to the square root of the number of events. (*Inset*) $\tilde{a}^4 P(\tilde{a})$ for the DNS data (*crosses*) and the multifractal prediction. Panel *b* reprinted with permission from Biferale et al., "Multifractal statistics of Lagrangian velocity and acceleration in turbulence," *Phys. Rev. Lett.*, 93:064502 (2004). Copyright (2004) by the American Physical Society.

Other experimental techniques provided access to velocity increments along tracer trajectories: Velocity differences at very small time gaps provide a signal closely related to acceleration. Mordant et al. (2002) have performed pioneering measurements in these directions. The dramatic change of PDF shape seen in **Figure 5*a*** provides an immediate impression of how strongly intermittent Lagrangian turbulence is at small time increments.

Numerically, tracer acceleration has been measured in many investigations (Biferale & Toschi 2005, Biferale et al. 2004a, Ishihara et al. 2007, Lee & Lee 2005, Yeung & Pope 1989). **Figure 4*b*** shows the results from a recent numerical simulation of Lagrangian tracers (Biferale et al. 2004a). The experimental and numerical data shown in **Figure 4** are normalized but, as they correspond to two different Reynolds numbers, cannot be superimposed. Indeed both the variance and the whole PDF of the acceleration carry an *Re* dependence (Biferale et al. 2004a).

Mordant et al. (2004a) carefully compared several theoretical models for the acceleration PDF against high–Reynolds number experimental data. Their results are shown in **Figure 4*a***; the MF model provides the best fit to the experimental data. Although the acceleration is measured in experiments by tracking a neutral particle, the local value of the acceleration is strictly an Eulerian quantity (equal to the material derivative of the velocity or the right-hand side of the Navier-Stokes equation), and the strongest contribution to the acceleration comes from the pressure gradient (Biferale & Toschi 2005, Vedula & Yeung 1999).

The MF formalism has been employed to describe the PDF of acceleration (Arimitsu & Arimitsu 2004, Biferale et al. 2004a, Chevillard et al. 2003) and the tightly related statistics of

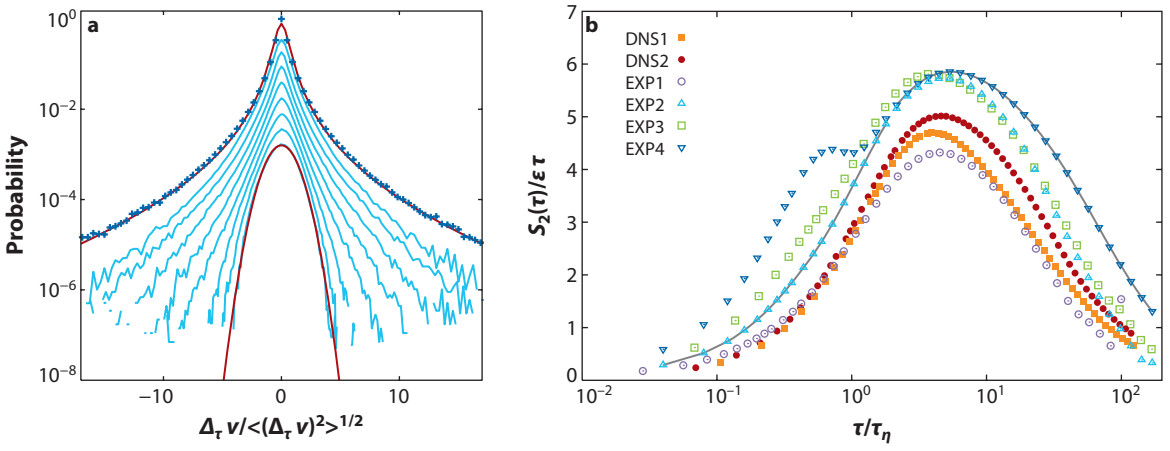

Figure 5

(*a*) Probability distribution function P of velocity increment Δv_τ calculated for time lags $100\tau/T_L = \{1.3; 2.7; 5.4; 11.2; 22.4; 44; 89.3; 174\}$. The curves are displayed with a vertical shift for clarity. Crosses correspond to a model prediction. Panel *a* reprinted with permission from Mordant et al., "Long time correlations in Lagrangian dynamics: a key to intermittency in turbulence," *Phys. Rev. Lett.*, 89(25):254502 (2002). Copyright (2002) by the American Physical Society. (*b*) Log-lin plot of the second-order Lagrangian velocity structure functions normalized with the dimensional prediction [i.e., $S_2(\tau)/(\varepsilon\tau)$] at various Reynolds numbers (see Biferale et al. 2008, tables 1 and 2). EXP2 and EXP4 refer to two experiments with the same Reynolds numbers ($R_\lambda = 690$) but with different measurement volumes (EXP4 has a larger measurement volume). In particular, EXP2 and EXP4 better resolve the small and large time-lag ranges, respectively, and intersect at $\tau/\tau_\eta \approx 2$. The solid line indicates the resulting data set comprising data from EXP2 (for $\tau/\tau_\eta < 2$) and EXP4 (for $\tau/\tau_\eta > 2$). A good overlap among these data is observed in the range $2 < \tau/\tau_\eta < 8$. For all data sets, an extended plateau is absent, indicating that the power-law regime typical of the inertial range has not been achieved, even at the highest Reynolds number, $R_\lambda \sim 815$, in experiment. Panel *b* reprinted with permission from Biferale et al., "Lagrangian structure functions in turbulence: a quantitative comparison between experiment and direct numerical simulation," *Phys. Fluids*, 20(6):065103 (2008). Copyright 2008, American Institute of Physics.

velocity increments (Mordant et al. 2004c). As shown in **Figure 4*b***, the expression for the acceleration (Equation 7) is in excellent agreement with numerical measurements. It is remarkable that it is possible to describe the PDF of the acceleration based purely on the knowledge of the statistical properties of Eulerian turbulence.

To better quantify the statistical properties of tracer dynamics, one can study conditioned statistical quantities. An example that we do not detail here is the PDF of acceleration conditioned on the absolute value of velocity, $P(a|v)$, a typical quantity of interest in stochastic modeling (Biferale & Toschi 2005, Crawford et al. 2005, Sawford et al. 2003).

3.2. Lagrangian Structure Functions of Velocity

Statistical properties of Lagrangian turbulence are best studied by means of temporal correlations, the simplest of which are the LVSFs defined as

$$S_p(\tau) = \langle [v_i(t+\tau) - v_i(t)]^p \rangle, \tag{4}$$

where i is a Cartesian component (i.e., x, y, or z). The corresponding Eulerian quantities (i.e., the moments of the spatial velocity increments) have been studied in depth (see Frisch 1995).

Within Kolmogorov's theory, in the inertial range in which the only physically relevant parameter is the rate of energy dissipation per unit mass ε, the second-order velocity moment is predicted to scale linearly versus the time separation $S_2(\tau) \simeq C_0\varepsilon\tau$ (e.g., see Monin & Yaglom 1975).

[We recall that this relation does not rest on solid ground as does the 4/5 power law for the Eulerian structure function of order 3, which can be derived exactly from the Navier-Stokes equations under mild hypotheses (Frisch 1995).] To date, the Reynolds numbers achieved in experiments and numerical simulations are too small to observe a sufficient scaling range to confirm this prediction (see **Figure 5*b***). However, DNS (Yeung et al. 2006) and experiments (Ouellette et al. 2006b) have observed the tendency for a plateau to develop as the Reynolds number is increased. Ouellette et al. (2006b) demonstrated that large-scale flow anisotropies influence C_0. They found a 30% variation among different velocity components, with little change with increasing Reynolds number. No other experimental data on the effect of large-scale anisotropies on Lagrangian turbulence are currently available (for a pioneering experiment dealing with the effects of flow on homogeneities, see Gerashchenko et al. 2008), but the effects of a stably stratified turbulent flow have recently been investigated numerically (van Aartrijk & Clercx 2008, van Aartrijk et al. 2008). The estimate for C_0 is between 3 and 7 and increases (but saturates) at increasing Reynolds numbers (Ouellette et al. 2006b).

The higher-order temporal structure functions deviate even stronger from the dimensional predictions than their Eulerian counterpart, as found in experiment (Mordant et al. 2001, Xu et al. 2006a) and DNS (Biferale & Toschi 2005, Biferale et al. 2004b). LVSFs are the moments of the PDF of Lagrangian velocity increments across a time delay τ, and the full PDFs were also studied by Mordant et al. (2002) and Chevillard et al. (2003), validating the MF model with success against experimental and numerical data (see **Figure 5*a***).

In the attempt to quote a single number for the inertial-range scaling properties of Lagrangian turbulence, first published results from experiments (Mordant et al. 2001, Xu et al. 2006a) and DNS (Biferale & Toschi 2005, Biferale et al. 2004b) performed fits in different time intervals obtaining somewhat different numbers (Bec et al. 2006c). It was shown recently that a much more refined analysis is possible, and experiments and DNS do indeed agree over the whole range of time delays (Arneodo et al. 2008, Biferale et al. 2008).

3.2.1. Quantitative comparison between experiments and simulations. An observable sensitive to intermittency in turbulence is the logarithmic derivative of structure functions. When applied to LVSFs, it reads

$$\zeta_i(p,\tau) = \frac{\mathrm{d}\,\log S_i^{(p)}(\tau)}{\mathrm{d}\,\log S_i^{(2)}(\tau)}. \tag{5}$$

The quantities $\zeta_i(p,\tau)$ [or $\zeta_p(\tau)$ when not specifying the component] have the meaning of local (i.e., at scale τ) scaling exponents. In the above definition, the derivative of $S^{(p)}$ is not taken with respect to τ but with respect to $S^{(2)}$ in the spirit of extended self-similarity (Benzi et al. 1993). [For Eulerian velocity structure functions, extended self-similarity extends considerably the scaling from the inertial range to the dissipative scales (Benzi et al. 1993).] The presence of a plateau for $\zeta_i(p,\tau)$ implies the existence of a range in which structure functions scale homogeneously.

To our knowledge, the earliest measurement of these quantities in the Lagrangian domain was reported in numerical simulations by Mazzitelli & Lohse (2004) and Biferale et al. (2004a). Arneodo et al. (2008) and Biferale et al. (2008) recently compared results from experiment and DNS. **Figure 6** shows the exponents $\zeta_p(\tau)$ for $p = 4$ and $p = 6$. An excellent agreement between numerical and experimental data is found from the dissipative scales up to the largest resolved scale (which, in the case of experiments, is smaller than the integral scale because of the limitation of the observation volume used).

A remarkable feature of Lagrangian turbulence is the dip at scales between the dissipative scales and the largest scales (see Arneodo et al. 2008; Biferale et al. 2004a, 2008; Mazzitelli &

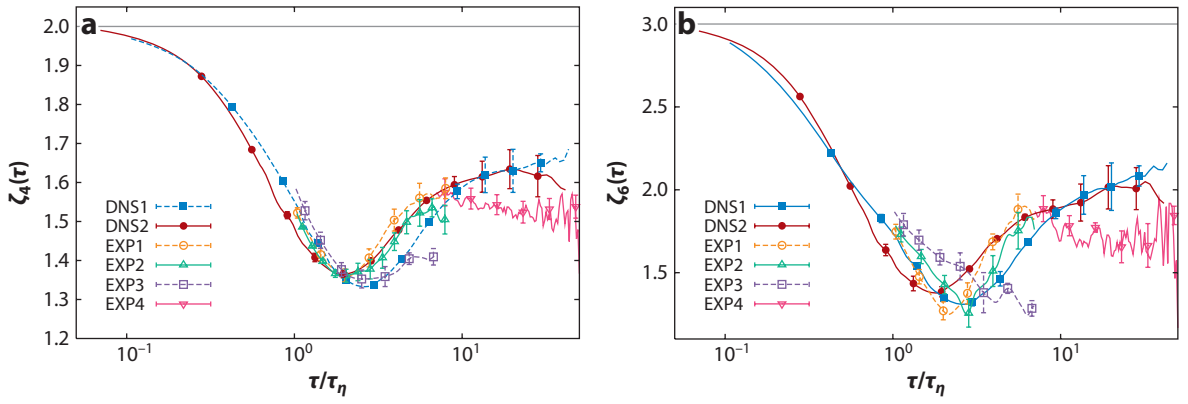

Figure 6

Logarithmic derivatives $\zeta_p(\tau)$ of structure functions $S_p(\tau)$ with respect to $S_2(\tau)$ for orders (*a*) $p = 4$ and (*b*) $p = 6$. The curves are averaged over the three velocity components, and the error bars are computed from the statistical (anisotropic) fluctuations between Lagrangian velocity structure functions of the different $i = x, y$, and z components. The horizontal lines are the nonintermittent values for the logarithmic local slopes (i.e., $\zeta_p = p/2$). The curves for EXP1, -2, and -3 are shown in the time range $1 \leq \tau/\tau_\eta \leq 7$, whereas the curves for EXP4 (large measurement volume) are shown in the time range $7 \leq \tau/\tau_\eta \leq 50$. Figure reprinted with permission from Biferale et al., "Lagrangian structure functions in turbulence: a quantitative comparison between experiment and direct numerical simulation," *Phys. Fluids*, 20(6):065103 (2008). Copyright 2008, American Institute of Physics.

Lohse 2004). This dip is seen in **Figures 6** and **7**, and its presence has been clearly associated with small-scale vortex filaments (Bec et al. 2006c). This conclusion relies on the observation that the dip disappears (*a*) when a sliding average of duration ≈ 1–$10\tau_\eta$ is applied to the fluid particle velocity or (*b*) for inertial particles significantly heavier than the fluid particles (heavy particles are expelled from vortex filaments; see Section 4).

Biferale et al. (2008) discussed quantitatively systematic effects and statistical uncertainties for both experiments and simulations. The systematic effects include large-scale anisotropies and finite durations of trajectories in experiments, whereas interpolation errors at very small space and timescales and the effect of periodic boundaries need to be considered for DNS. Statistical uncertainties are primarily related to the finite number of particle trajectories and additionally, for DNS, to the duration of the simulation. DNS can help quantify the effect of some geometrical and statistical effects present in the experiment, but as DNS has lower Reynolds numbers, it also has a smaller inertial range than experiments.

3.2.2. Universality. To test the universality of Lagrangian turbulence, Arneodo et al. (2008) compared three different experiments and five different numerical simulations. Similar to Biferale et al. (2008), they extracted the local scaling exponents by means of their definition (Equation 5) and compared those exponents scale by scale in those ranges in which each data set was presumed to yield sufficiently accurate results. Although the data covered a wide range of Reynolds numbers and came from different experimental and numerical setups, all data collapsed on one curve. This suggests a universality in the physics of Lagrangian turbulence over the whole range of time lags.

Arneodo et al. (2008) also compared the experimental and numerical data with an MF prediction and found excellent agreement (**Figure 7**). They used a modification of the MF model, initially proposed by Chevillard et al. (2003), capable of interpolating smoothly all the way from the inertial range down to the dissipative scales.

An important observation is that Eulerian velocity statistics can be measured in terms of longitudinal or transverse velocities, whereas the fluid velocity along particle trajectories is probably

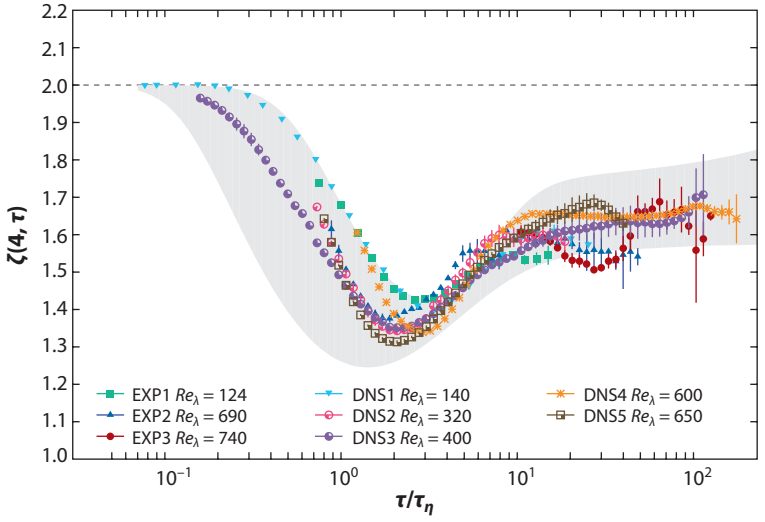

Figure 7

Log-lin plot of the fourth-order local exponent, $\zeta(4, \tau)$, averaged over the three velocity components, as a function of the normalized time lag τ/τ_η. Data sets come from three experiments (EXP1–3) and five direct numerical simulations (DNS1–5). Error bars are estimated from the spread among the three components, except in EXP3, in which only two components were measured. Each data set is plotted only in the time range in which the known experimental/numerical limitations certainly do not affect the results. In particular, for each data set, the largest time lag always satisfies $\tau < T_L$. The minimal time lag is set by the highest fully resolved frequency. The shaded area displays an envelope of the prediction obtained by the multifractal model by using both $D_L(h)$ and $D_T(h)$, with $\beta = 4$, for a range of $R_\lambda \in [150, 800]$, comparable with the range of Reynolds numbers in the data. The straight dashed line corresponds to the dimensional nonintermittent value $\zeta(4, \tau) = 2$. Notice that two DNS are sufficiently resolved to achieve the right dimensional scaling in the high-frequency limit. Figure reprinted with permission from Arneodo et al., "Universal intermittent properties of particle trajectories in highly turbulent flows," *Phys. Rev. Lett.* 100(25):254504, 2008. Copyright (2008) by the American Physical Society.

mixing both velocity statistics. The envelope of prediction obtained by the MF model shown in **Figure 7** is obtained by evaluating the LVSF using the Eulerian fractal dimensions $D_L(h)$ and $D_T(h)$ obtained by fitting longitudinal (Arneodo et al. 1996) and transverse (Gotoh et al. 2002) Eulerian velocity structure functions, respectively. For more details, we refer the reader to Arneodo et al. (2008).

3.3. Other Statistics

This section deals with particle dispersion and the statistics of trajectories of particles initially released from nearby locations.

3.3.1. Pair dispersion. A particularly important issue in Lagrangian turbulence is the relative evolution of a particle cloud. In its simplest terms, it is represented by the separation of pairs of particles carried along their trajectories (for further details, see Salazar & Collins 2009). Although the study of two-particle relative separation has attracted much attention (e.g., see Biferale et al. 2005a, 2006; Bourgoin et al. 2006; Ouellette et al. 2006a), the focus shifted recently to the evolution of higher-order correlations such as tetrahedral shapes in turbulence (i.e., the evolution of a set

of four particles) (Biferale et al. 2005b; Chertkov et al. 1999; Lüthi et al. 2007; Pumir et al. 2000; Xu et al. 2007b, 2008).

3.3.2. Shape evolution. The evolution of tetrads in turbulence can provide important information on velocity gradients (Biferale et al. 2005b; Chertkov et al. 1999; Lüthi et al. 2007; Xu et al. 2007b, 2008). **Figure 8*a*** shows a typical configuration of a tetrad subset out of the evolution of a total of 9.6×10^4 tetrads numerically integrated at $R_\lambda \sim 280$ (Biferale et al. 2005b).

The geometrical shape of a tetrad can be characterized in terms of its size r and the eigenvalues of the moment of inertia tensor denoted by g_i ($g_1 \geq g_2 \geq g_3$). **Figure 8*b*** shows the temporal growth of g_1, g_2, and g_3; unfortunately, the finite resolution does not allow for a clean identification of the temporal scaling behavior. Recent experiments studied the same quantities (e.g., see Xu et al. 2007b, 2008), and results are in agreement with numerical simulations. Small differences are probably associated with the restriction of the initial size of tetrads to the inertial range in experiments

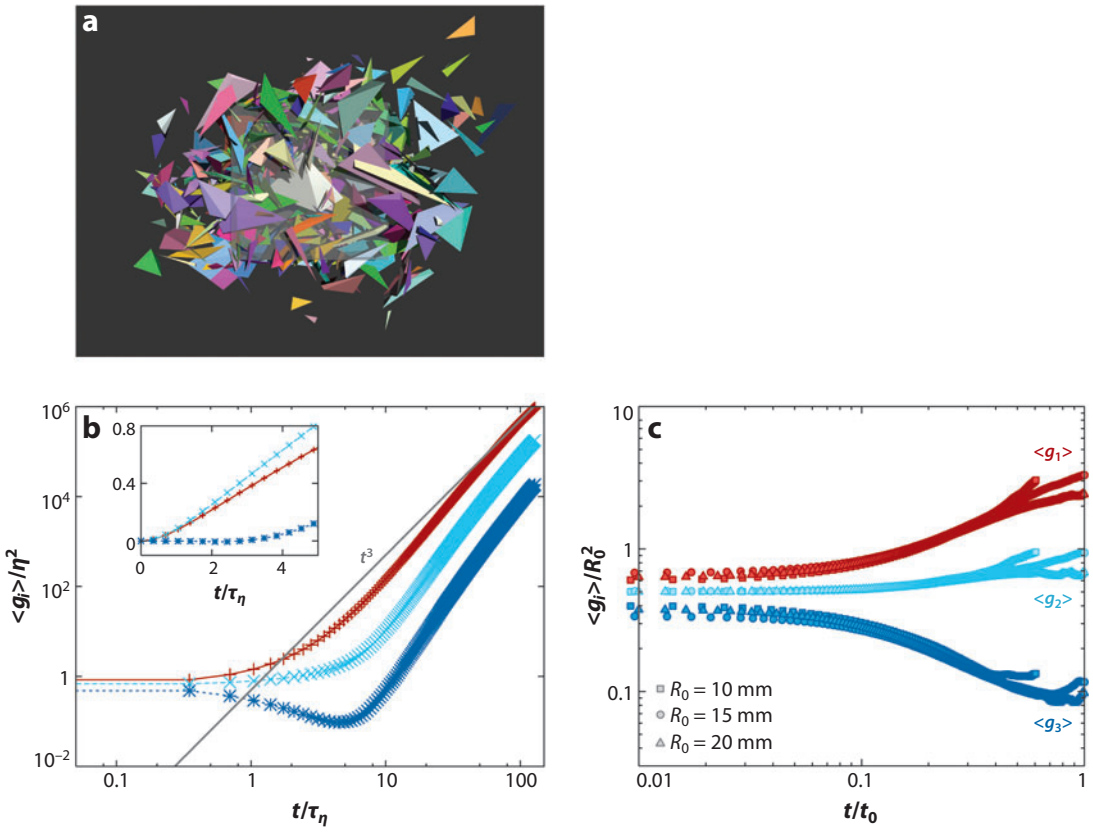

Figure 8

(*a*) Snapshot at $t = 0.65T_L$ of 480 tetrahedra evolving in the turbulent flow starting from regular tetrahedra at the Kolmogorov scale. (*b*) Evolution of the mean eigenvalues g_1 (*plus signs*), g_2 (*multiplication signs*), and g_3 (*asterisks*) of the moment of the tensor of inertia. The line represents the dimensional scaling t^3. (*Inset*, *from top to bottom*) Evolution at small times of $\langle \ln A(t) \rangle$ (surface), $\langle \ln R(t) \rangle$ (distance), and $\langle \ln V(t) \rangle$ (volume). Figure reprinted with permission from Biferale et al., "Multiparticle dispersion in fully developed turbulence," *Phys. Fluids*, 17:111701, 2005. Copyright 2005, American Institute of Physics. (*c*) Evolution of Lagrangian tetrads from an experiment at $R_\lambda = 690$ ($\eta = 30$ μm) from an experiment. The eigenvalues of the tensor of inertia are scaled by the initial tetrad size. Figure reproduced from *New J. Phys.* 10(1) Xu et al. (2008) with permission of IOP Publishing Ltd.

(see **Figure 8*c***). As already shown by Chertkov et al. (1999) for lower Reynolds numbers, tetrads deform under the action of turbulence and become elongated and almost coplanar objects.

3.4. Modeling

Owing to the availability of Lagrangian data, there have been several attempts at developing, testing, and improving analytical models. We recall the MF model (Parisi & Frisch 1985), the tetrad model pioneered by Chertkov et al. (1999), the models based on superstatistics (discussed in Gotoh & Kraichnan 2004, Mordant et al. 2004b), and vortex models (Zybin et al. 2008). Here we restrict the discussion to the MF model (Benzi et al. 1984, Boffetta et al. 2008, Parisi & Frisch 1985), which has proven to be capable of describing many different features of Eulerian turbulence (including those as complex as multitime and multiscale correlations; see Biferale et al. 1999). Borgas (1993) suggested an extension of the MF model to the Lagrangian domain but observed that no reliable data were available at the time to test its validity. Today the MF model has been extended and tested on the acceleration PDF for tracers and on the all-scale behavior of LVSFs. Models based on superstatistics have also been employed to fit the acceleration PDF and to predict scaling exponents (Arimitsu & Arimitsu 2004, Beck 2007) with different degrees of success (Mordant et al. 2004b).

In recent years, many groups have explored the possibility of abridging the MF model to the temporal domain (Biferale et al. 2004a, 2005c; Boffetta et al. 2002; Borgas 1993; Chevillard et al. 2003; Homann et al. 2007b; Mordant et al. 2001; Xu et al. 2006b).

Chevillard et al. (2003) presented and validated one of the first comparisons among MF model and experimental and numerical data, all the way from dissipative to inertial scales. Later Biferale et al. (2004a) demonstrated the possibility of remapping the Eulerian MF formalism onto the Lagrangian one. The main advantage here is that one can virtually make a prediction without any new free parameter, once the statistical properties of Eulerian turbulence are known (e.g., measured) (Arneodo et al. 2008).

In the MF formalism, the global-scale invariance of Kolmogorov's (1941) theory becomes a local-scale invariance; namely, the turbulent flow is assumed to possess a range of scaling exponents $\mathcal{I} = (h_{\min}, h_{\max})$. For each $h \in \mathcal{I}$, there is a set $\mathcal{S}_h \in \boldsymbol{R}^3$ of fractal dimension $D(h)$ such that, in the limit of small r, $\delta_r u(\boldsymbol{x}) \sim u_0 (r/L_0)^{h(\boldsymbol{x})}$ for $\boldsymbol{x} \in \mathcal{S}_h$, where u_0 is the large-scale fluctuating velocity and L_0 is the integral length scale. The scaling properties of the Eulerian structure function are derived by integrating over all possible h (see Frisch 1995): $\langle (\delta_r u)^p \rangle \sim \langle u_0^p \rangle \int_I dh (r/L_0)^{hp+3-D(h)}$. The factor $(r/L_0)^{3-D(h)}$ is the probability of being within a distance of order r from the set $\mathcal{S}_h$ of dimension $D(h)$. A saddle-point approximation in the limit $r \ll L_0$ then gives the scaling exponents $\zeta_E(p) = \inf_h [hp + 3 - D(h)]$. If the Eulerian scaling exponents ζ_p are known, one can calculate $D(h)$ from the inverse of the Legendre transformation. The velocity fluctuations along a particle trajectory may be considered as the superposition of different contributions from eddies of all sizes. In a time lag τ, the contributions from eddies smaller than a given scale, r, are uncorrelated, and one can write $\delta_\tau v \sim \delta_r u$. The presence of fluctuating eddy turnover times is the only extra ingredient introduced by MF formalism in the Lagrangian reference frame. One can derive the expression for LVSFs

$$\mathcal{S}_p(\tau) \sim \int_h \mathrm{d}h \, \delta v_\tau^p(h) \mathcal{P}(\tau, T_L; h) = \langle v_0^p \rangle \int_{h \in I} \mathrm{d}h \left(\frac{\tau}{T_L} \right)^{\frac{hp+3-D(h)}{1-h}}, \tag{6}$$

where $\delta v_\tau(h) = v_0 (\tau / T_L)^{h/(1-h)}$ and $\mathcal{P} = (\tau / T_L)^{[3-D(h)]/(1-h)}$ (Boffetta et al. 2002). The Lagrangian scaling exponents $\zeta_L(p)$ then follow from a saddle-point approximation in the limit $\tau \ll T_L$;

$\zeta_L(p) = \inf_h \left(\frac{hp+3-D(h)}{1-h}\right)$. One can use the $D(h)$ of the She-Lévêque model to obtain the following estimates: $\zeta_L(4)/\zeta_L(2) = 1.71$, $\zeta_L(6)/\zeta_L(2) = 2.16$, and $\zeta_L(8)/\zeta_L(2) = 2.72$ (Biferale et al. 2004a).

One can use a similar phenomenological argument to derive predictions for statistical properties of the acceleration, which can be defined as $a \equiv \frac{\delta_{\tau_\eta} v}{\tau_\eta}$. The final expression derived in Biferale et al. (2004a), after normalizing the acceleration $\tilde{a} = a/\sigma_a$ with its variance $\sigma_a = \langle a^2 \rangle^{1/2}$, is

$$\mathcal{P}(\tilde{a}) \sim \int_{h \in I} \tilde{a}^{\frac{[h-5+D(h)]}{3}} R_\lambda^{y(h)} \exp\left(-\frac{1}{2}\tilde{a}^{\frac{2(1+h)}{3}} R_\lambda^{z(h)}\right), \tag{7}$$

where $y(h) = \chi[h - 5 + D(h)]/6 + 2[2D(h) + 2h - 7]/3$, $z(h) = \chi(1 + h)/3 + 4(2h - 1)/3$, and $\chi = \sup_h\{2[D(h) - 4h - 1]/(1 + h)\}$.

To interpolate smoothly to the dissipative behavior $\langle \delta v^n(\tau) \rangle \sim \tau^n$ for $\tau \ll \tau_\eta$, Chevillard et al. (2006) and Arneodo et al. (2008) used the following expression: $\delta_\tau v(h) = v_0 \frac{\tau}{T_L}[(\frac{\tau}{T_L})^\beta + (\frac{\tau_\eta}{T_L})^\beta]^{\frac{2h-1}{\beta(1-h)}}$, where β is a free parameter controlling the crossover around $\tau \sim \tau_\eta$. The expression for the LVSF is given by Equation 6, which considers the intermittent fluctuations of the dissipative scale $\tau_\eta(h)/T_L \sim R_\lambda^{2(h-1)/(1+h)}$ (Biferale et al. 2004a, Borgas 1993). The probability for observing a scaling exponent h is estimated in analogy with Equation 6, $P_h(\tau, \tau_\eta) = \mathcal{Z}^{-1}(\tau)[(\frac{\tau}{T_L})^\beta + (\frac{\tau_\eta}{T_L})^\beta]^{\frac{3-D(h)}{\beta(1-h)}}$, with a normalizing function $\mathcal{Z}$ and $D(h)$ indicating again the Eulerian fractal dimension. For a given Reynolds number, the model has two free parameters, namely β and a multiplicative constant in the definition of τ_η, plus the known function $D(h)$ (Arneodo et al. 2008).

4. MORE COMPLEX REALIZATIONS AND FUTURE DIRECTIONS

After having considered the dynamics of fluid tracers in turbulence, it is natural to wonder what happens to particles having a density ρ_p different from that of the advecting fluid ρ_f. The simplest case, in which the particle size is much smaller than the Kolmogorov scale of turbulence, has recently received much attention and has brought interesting results. A commonly used model for passively advected particles (sufficiently dilute to neglect a back-reaction on the flow and collisions among particles) follows from Auton et al. (1988), Babiano et al. (2000), Gatignol (1983), and Maxey & Riley (1983). The equations are expected to hold in turbulent flows as long as the particle size is much smaller than the Kolmogorov length scale, as then the particles locally see a Stokes flow. Notably, recent experimental investigations have started to explore the effects of finite-particle size: This should be useful in validating the numerical models (Qureshi et al. 2007, Voth et al. 2001). In the numerical description, it is also common to neglect the lift force (Van Nierop et al. 2007) and memory terms. The settling of particles in a turbulent flow under gravity has recently received much attention (see Bosse et al. 2006, van Aartrijk & Clercx 2008). Because of their inertia, measured by the Stokes time $\tau = a^2/(3\beta\nu)$ [where a is the particle radius, ν is the fluid viscosity, and $\beta = 3\rho_f/(2\rho_p + \rho_f)$], particles depart from fluid streamlines and distribute nonhomogeneously (see Balkovsky et al. 2001, Crisanti et al. 1992, Maxey 1987) (**Figure 9**). Dependent on the density ratio β, particles probe different flow structures: Light particles ($\beta > 1$; e.g., air bubbles in water) preferentially concentrate in regions of high vorticity, a property also used in flow visualization (Douady et al. 1991) and the study of cavitation (La Porta et al. 2000). Heavy particles ($\beta < 1$; e.g., a water droplet in air) are expelled from rotating regions. The strength of such a differential response to flow structures and the consequent segregation of particles having different densities also depend quantitatively on the actual value of the Stokes number $St = \tau/\tau_\eta$ (see Calzavarini et al. 2008a,b; Saw et al. 2008; Sundaram & Collins 1999; and references therein).

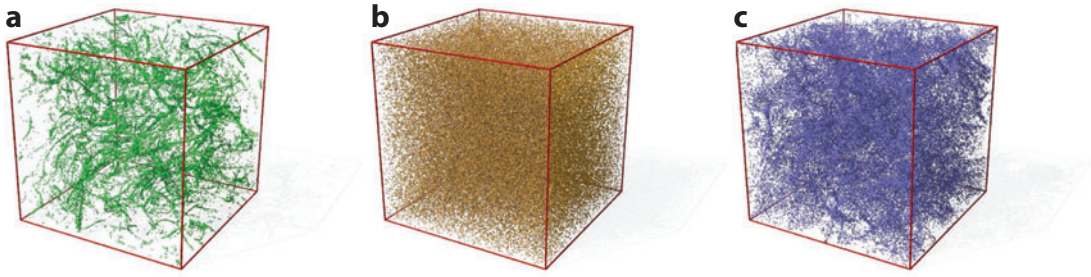

Figure 9

Snapshots of particle distributions in a turbulent flow field at $St = 0.6$ for (*a*) $\beta = 3$ (bubbles), (*b*) $\beta = 1$ (tracers), and (*c*) $\beta = 0$ (heavy particles). Corresponding videos can be downloaded with the online version of Calzavarini et al. 2008b. Figures reprinted with permission from Calzavarini et al., "Minkowski functionals: characterizing particle and bubble clusters in turbulent flow," *J. Fluid Mech.*, 607:13–24, 2008. Copyright (2008) Cambridge University Press.

4.1. Heavy Particles

One important difference between fluid tracers and particles is that the effective velocity field of the latter is compressible (i.e., particles can accumulate). In fact their velocity field is compressible even when advected by a solenoidal velocity field (Falkovich & Pumir 2004).

Because of the qualitatively different behavior of heavy and light particles (i.e., particles that are denser or less dense than the fluid), we discuss first the most-studied case of heavy particles. A prominent feature of heavy particles is that they show the phenomenon of preferential concentration, which has been studied extensively in the past (see Balkovsky et al. 2001, Eaton & Fessler 1994, Salazar et al. 2008, Saw et al. 2008, Squires & Eaton 1991, Yang & Shy 2005). Only recently, owing to rapid developments in experimental Lagrangian tracking techniques, has it become possible to investigate heavy-particle dynamics in laboratory flows at high Reynolds numbers (Ayyalasomayajula et al. 2006, Salazar et al. 2008, Saw et al. 2008, Voth et al. 2001). In numerical simulations, owing to the advancement in computational power, it has also become possible to numerically simulate the dynamics of inertial particles at higher Reynolds numbers (Bec et al. 2006a; Calzavarini et al. 2008b,c; Cencini et al. 2006). Whereas the first studies focused on characterizing the mass distribution of particles, the recent focus has been on fully characterizing the temporal evolution and correlating it with the properties of the underlying flow.

4.1.1. Acceleration. The acceleration of heavy particles shows decreasing intermittency with increasing Stokes numbers. Voth et al. (2001) found this in early experiments; however, the particles' size was larger than the Kolmogorov scale of the flow. Bec et al. (2006a) and Cencini et al. (2006) investigated this phenomenon as a function of Stokes number by numerically solving the equations of motion for point particles (discussed above) in a turbulent velocity field integrated by means of DNS.

Figure 10*b* shows the root-mean-squared acceleration as a function of Stokes number from Bec et al.'s (2006a) numerical simulation: Already for Stokes numbers as small as $St \sim 0.1$, the a_{rms} values drop by an order of 20%. The same plot also shows the root-mean-squared acceleration both of the fluid (conditioned to be) at the particle position and of filtered tracer trajectories. It is evident that the behavior for small Stokes numbers (up to 0.3) can be explained by preferential concentration effects, whereas for large Stokes values (i.e., St larger than 3.0), the filtering effect due to inertia can explain the observed behavior (for details, see Bec et al. 2006a). Recently, Ayyalasomayajula et al. (2006) measured experimentally the acceleration PDF for small particles.

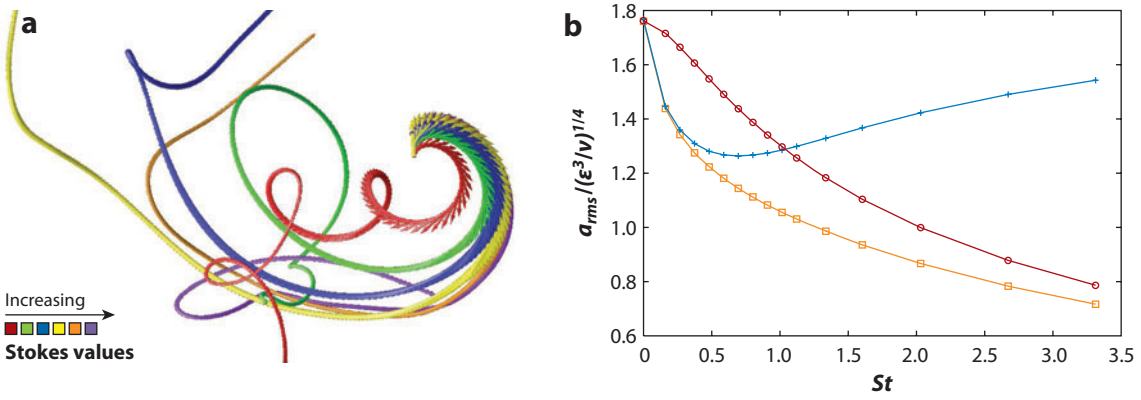

Figure 10

(*a*) Trajectories of heavy particles with different inertia. When released from within a small-scale vortex filament (matching the velocity of the underlying fluid), particles with different inertia respond to vorticity differently. Particles with large Stokes values, *St*, are almost insensitive to the presence of the vortex (the *red line* represents a fluid tracer, whereas the *green*, *blue*, *brown*, and *yellow lines* correspond to increasing Stokes values, respectively). (*b*) Comparison between the acceleration variance, a_{rms} (*squares*), as a function of Stokes value, with the acceleration of the fluid tracers measured at the particle position, $\langle(\frac{Du}{Dt}^F)^2\rangle^{1/2}$ (*plus signs*). The last curve (*circles*), approaching the a_{rms} for large *St*, is the one obtained from the filtered tracer trajectories, a^F_{rms}. All data are from a numerical simulation at $R_\lambda = 185$. Reprinted with permission from Bec et al., "Acceleration statistics of heavy particles in turbulence," *J. Fluid Mech.*, 550:349–58, 2006. Copyright (2006) Cambridge University Press.

Figure 11 compares these experimental data and results from numerical simulations. The agreement is quite satisfactory. A thorough discussion is given by Ayyalasomayajula et al. (2006), Bec et al. (2006a), Cencini et al. (2006), and Toschi et al. (2008). The acceleration of heavy particles has also been modeled with success as an autoregressive stochastic process (Sawford & Guest 1991) and more recently in terms of a stochastic distribution of point vortices (Ayyalasomayajula et al. 2008).

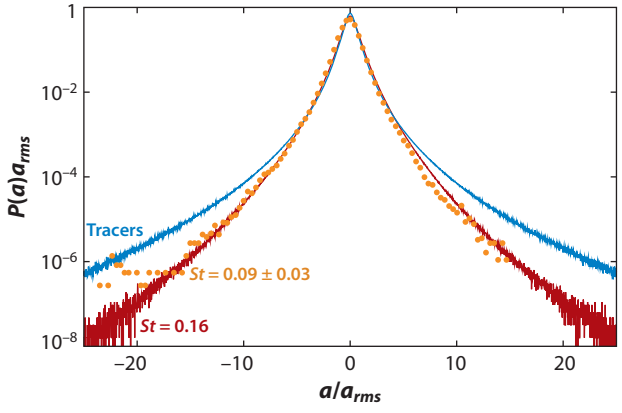

Figure 11

Lin-log plot, comparing an experimental acceleration probability distribution function for heavy particles at $St = 0.09 \pm 0.03$ (*circles*) (data from Ayyalasomayajula et al. 2006, courtesy of Zellman Warhaft), numerical data (*red solid line*) at $St = 0.16$ (Bec et al. 2006a, Cencini et al. 2006, Toschi et al. 2008), and numerical data for tracers (*blue solid line*) (Biferale et al. 2004a).

4.1.2. Lagrangian velocity structure functions. From LVSFs, one can clearly detect a strong signature of the tendency of heavy particles to be expelled from vortical regions. For increasing Stokes numbers, the LVSF loses the dip present for fluid tracers at time lags $\tau_\eta \in [1,\ 10]$ (Bec et al. 2006c). An important question is whether it is possible to describe the evolution of a concentration of heavy particles by means of a continuous field (i.e., to provide an Eulerian description for the evolution of swarms of heavy particles). Boffetta et al. (2007) recently performed an accurate quantitative test in this direction, concluding that for $St \geq 0.1$, sling effects are so important that a continuum description inevitably fails to reproduce the formation of shocks.

4.1.3. Preferential concentration. Particles do not remain uniformly distributed; hence it is of interest to investigate how to correlate their positions or velocities with Eulerian flow features. This may be particularly helpful in developing efficient computational models for Lagrangian transport. Recently, it was suggested that in two dimensions, the clustering of heavy particles may reflect the clustering of acceleration stagnation points, regardless of the Stokes number (Chen et al. 2006, Goto & Vassilicos 2006).

Bec et al. (2007) suggested a connection between acceleration and particle clustering. One way to properly characterize the small-scale clustering properties is by the fractal attractor for heavy particles; although experimentally quite difficult, Bec et al. (2006b) has accomplished this in numerical simulations.

4.2. Light Particles

The most ubiquitous light particles are bubbles in water. When small enough with respect to the turbulence dissipative scale, they can be considered nondeformable (Mazzitelli et al. 2003a,b), and, if the volume fraction is not too large, the back-reaction on the turbulent flow itself can be neglected (Calzavarini et al. 2008c). In their simplest modelization, light particles can be described in terms of Equation 3, in which the lift-force contribution has been neglected for simplicity (for more details on lift force, see Van Nierop et al. 2007).

4.2.1. Acceleration. An intriguing feature of light particles is that their acceleration variance can be larger than that of tracers, as found both in experiments (Volk et al. 2008a,b; Voth et al. 2001) and in numerical simulations (Volk et al. 2008a). For light particles, the added mass term proportional to the ratio of the fluid densities $\beta = 3\rho_f/(2\rho_p + \rho_f)$ can become important. A systematic investigation of the importance of the added mass term to acceleration is difficult in experiments, but possible in numerical simulations. **Figure 12*a*** shows the behavior of the root-mean-squared acceleration of light particles at varying β and St: The dominance of the added mass term for $St \geq 1$ and for large β is evident. The flatness of the acceleration (**Figure 12*b***) is most modified for $St \simeq 1$. The agreement shown between the acceleration PDF in DNS and experiments (**Figure 12*c***) is encouraging, especially when considering that the simulations used an oversimplified version of the equation of motion (e.g., the lift term was neglected) (Volk et al. 2008a,b).

4.2.2. Preferential concentration. Several tools can be used to characterize the space distribution of particles. Recently, a systematic quantitative exploration of the full parameter space (St, β) was possible thanks to numerical databases. **Figure 13*a*** illustrates the Kaplan-Yorke dimension of the attractor [defined as $d_{KY} = K + \sum_{i=1}^{K} \lambda_i/|\lambda_{K+1}|$, where K is the largest integer such that $\sum_{i=1}^{K} \lambda_i > 0$ and $\lambda_1 \geq \lambda_2 \cdots \geq \lambda_6$ represent the Lyapunov exponents (Ott 2002)]. The Kaplan-Yorke dimension of the attractor can be considered an interpolated dimension for which

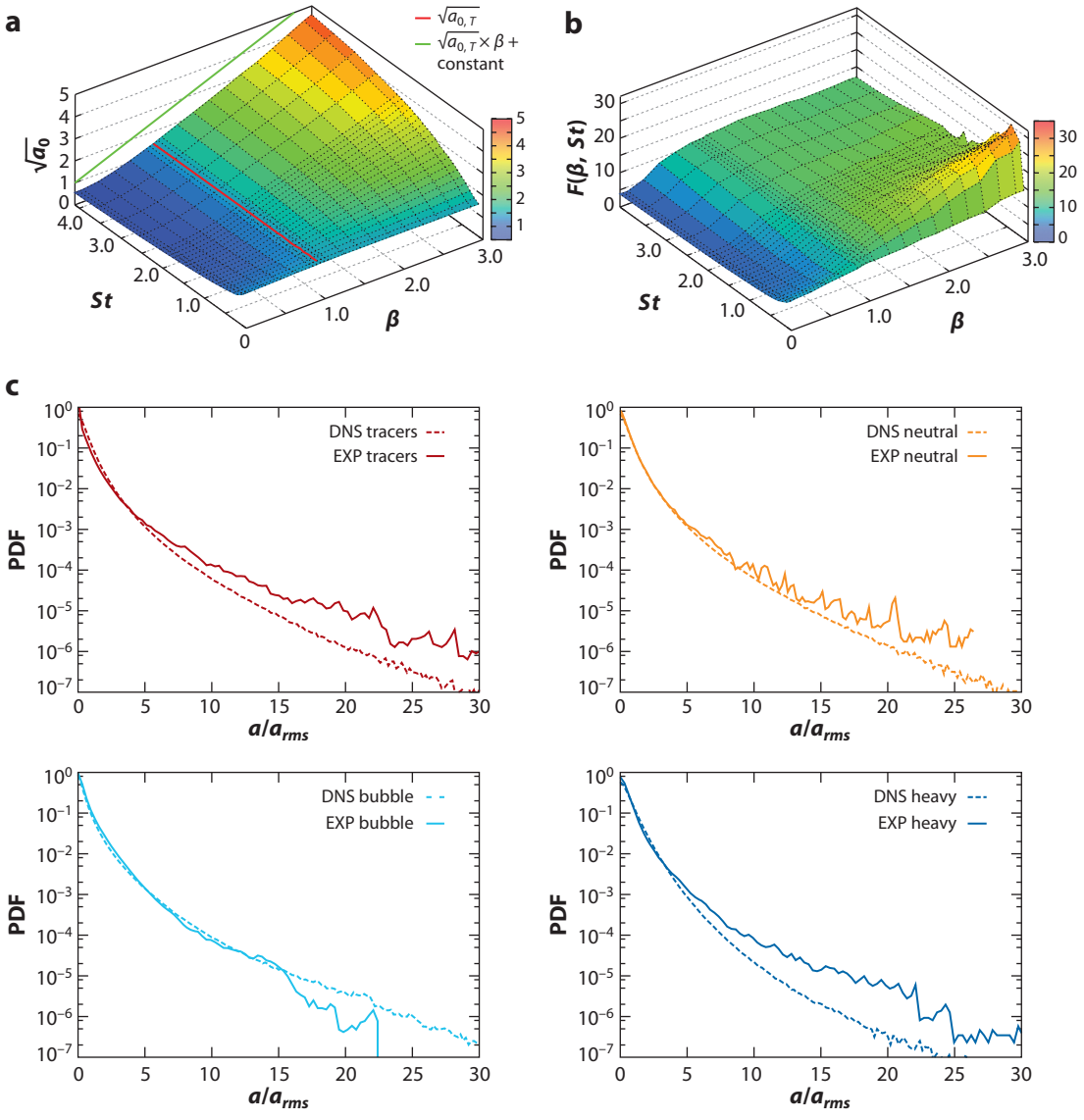

Figure 12

(*a*) The behavior of the normalized root-mean-squared acceleration $\sqrt{a_0} = (\langle a^2 \rangle \varepsilon^{-3/2} \nu^{1/2})^{1/2}$ as a function of both *St* and β for an $R_\lambda = 75$ direct numerical simulation (DNS). Isocontours for $\sqrt{a_{0,T}}$ (*red*) and the line $\sqrt{a_{0,T}} \cdot \beta + const.$ (*green*) are also reported. Note that a_0 does not depend on *St* for neutral ($\beta = 1$) particles, whereas it is always reduced/enhanced for heavy/light particles. For large particles ($St \simeq 4.1$), $\sqrt{a_0} \simeq \beta \sqrt{a_{0,T}}$. (*b*) The flatness of acceleration $\mathcal{F} = \langle a^4 \rangle / \langle a^2 \rangle^2$ as a function of both *St* and β, data from the same numerical simulation. (*c*) Probability distribution function (PDF) of accelerations, normalized to their variance, comparing experimental (EXP) measurements and DNS results: data from experiment at $R_\lambda = 850$, DNS of homogeneous isotropic turbulence at $R_\lambda = 180$. Panels *a* and *c* reprinted from *Phys. D*, Vol. 237, Volk et al., "Acceleration of heavy and light particles in turbulence: comparison between experiments and direct numerical simulations," pp. 2084–89, copyright (2008), with permission from Elsevier.

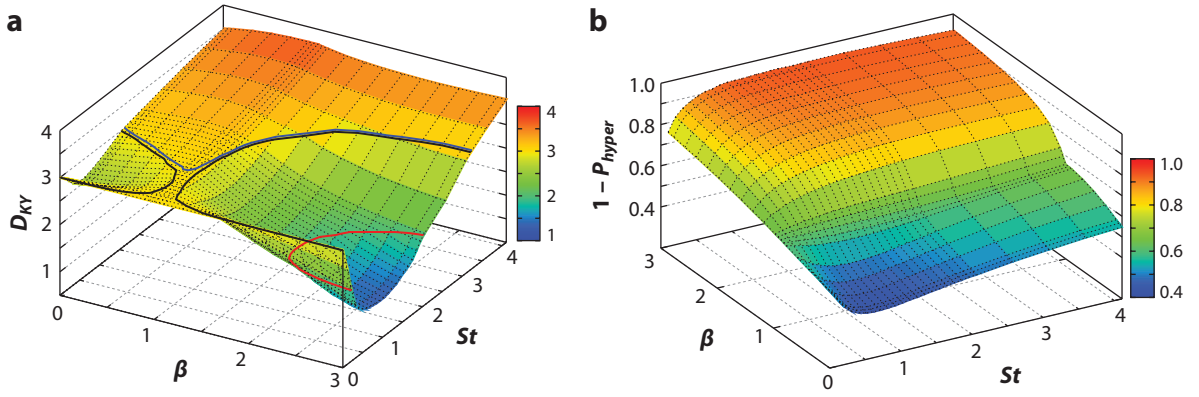

Figure 13

(*a*) The Kaplan-Yorke dimension d_{KY} as a function of both β and St. Light particles, as compared with heavy particles, have a much stronger tendency to evolve on attractors with smaller fractal dimensions. Panel *a* reprinted with permission from Calzavarini et al., "Minkowski functionals: characterizing particle and bubble clusters in turbulent flow," *J. Fluid Mech.*, 607:13–24, 2008. Copyright (2008) Cambridge University Press. (*b*) Probability of finding a particle in a rotational region ($1 - P_{hyper}$) as a function of both β and St. As soon as particles are lighter than the advecting fluid, they tend to remain in rotational regions. For heavy particles, the opposite tendency (i.e., to stay in hyperbolic regions) is much less pronounced.

the dynamical evolution in phase space, on average, produces neither stretching nor shrinking. The dimension d_{KY} is measured by linearizing the dynamics (for full details, see, e.g., Bec 2003, Bec et al. 2006b, Calzavarini et al. 2008b).

Figure 13*a* presents a generalization (to the full β-St plane) of what Bec et al. (2006b) previously measured for heavy particles. In a finite region for $\beta \sim 3$, d_{KY} changes values from 2 to as small as 1.5, close to the values quoted by Moisy & Jiménez (2004) for the turbulent structures characterized by high dissipation. **Figure 13*b*** shows the probability of finding a particle in a location in which the strain matrix $\sigma_{ij} = \partial_i u_j$ possesses two complex conjugate eigenvalues (rotating regions; see Chong et al. 1990). The probability of finding light particles ($\beta > 1$) in such regions is close to unity.

If we compare the panels of **Figure 13**, we can see a clear correlation for heavy particles between the behavior of d_{KY} and the probability of being located in rotating regions. d_{KY} and P_{hyper} attain the minimum for similar values of St, and the overall shape of the curve is also quite close, suggesting a strong correlation between the clustering of heavy particles and the vortex ejection mechanism. However, this does not appear to be the case for light particles. Indeed, from values of St larger than those for which d_{KY} attains its minimum, the probability of having two complex conjugate eigenvalues stays constant to values $\mathcal{O}(1)$. This indicates that, regardless of the observed dimension, light particles stay in regions of the flow characterized by rotation.

A complete topological characterization of the space distribution of particles can be done in terms of Minkowski functionals (Calzavarini et al. 2008b). The basic idea is simple and consists of growing spheres centered around particles: When increasing the radius of the spheres, the topological object that emerges is increasingly space filling (see **Figure 14*a***). In an analysis based on the Minkowski functional, Calzavarini et al. (2008b) studied the four Minkowski invariants by changing the radii of the spheres. By analyzing the evolution of these quantities (e.g., contrasting with respect to a Poisson distribution), one can obtain quantitative information on the topology of the particle distribution. **Figure 14*b*** illustrates the typical behavior of the four invariants for tracers and heavy and light particles.

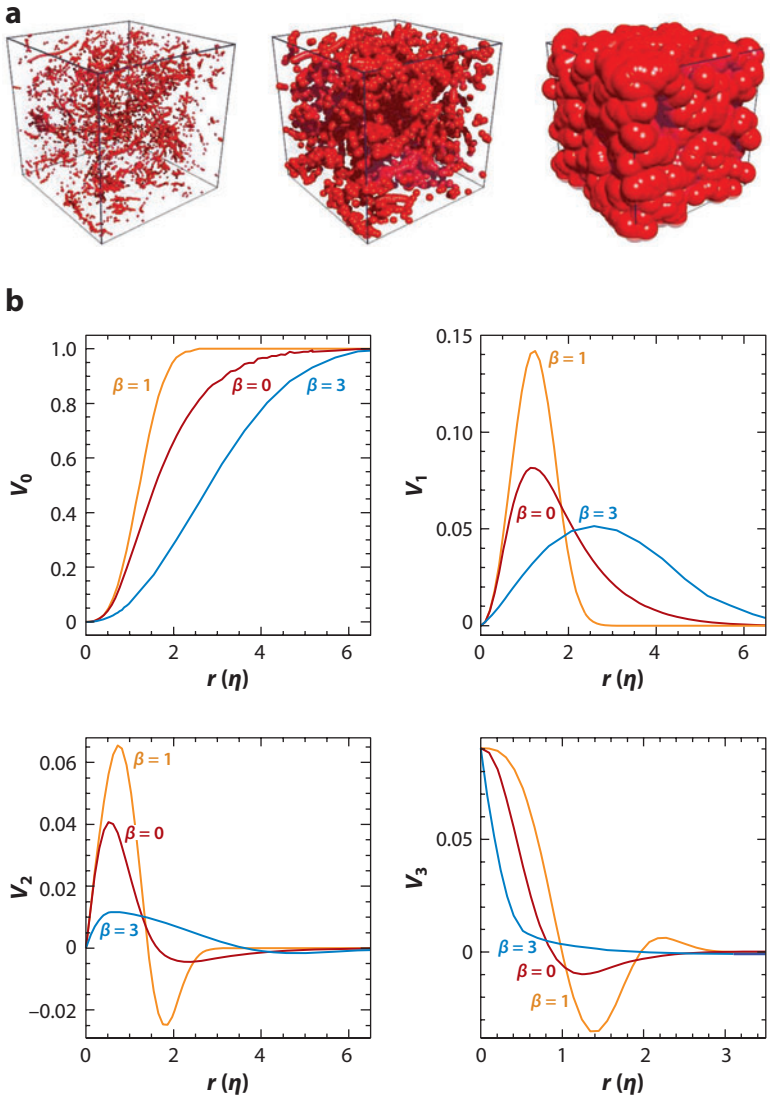

Figure 14

(*a*) Balls with radius r are grown on top of a particle distribution to compute the Minkowski functionals (from left to right, the radii are 1.25, 3.75, and 12.5, respectively). The characteristic results of the subsequent object are studied by means of the four Minkowski functionals (Calzavarini et al. 2008b). (*b*) Volume densities of the Minkowski functionals $v_\mu(r)$; $\mu = 0$, 1, 2, and 3; for passive tracers ($\beta = 1$, *orange*, corresponding to those of a Poisson distribution), heavy particles ($\beta = 0$, *red*), and bubbles ($\beta = 3$, *blue*). In all cases, $St = 0.6$ and $R_\lambda = 78$. Distances are in Kolmogorov's scale units (η). Figure reprinted with permission from Calzavarini et al., "Minkowski functionals: characterizing particle and bubble clusters in turbulent flow," *J. Fluid Mech.*, 607:13–24, 2008. Copyright (2008) Cambridge University Press.

5. OUTLOOK

Today it is possible to investigate the Lagrangian properties of turbulence at high spatial and temporal resolutions. Data-analysis tools are also becoming sufficiently refined to allow direct comparison of experiments and numerical simulations with models from the rapidly advancing field of theoretical analysis.

The understanding of many phenomena, rooted in the phenomenology of turbulence, is crucial to make any progress on both the fundamental and engineering fronts. The physics of real-world turbulence, however, includes shear, the difference in turbulence-generation mechanisms, and many other issues involving anisotropies and nonhomogeneities. Additionally, the situation can be even more complex for multiphase and particle-laden flows, in which particles may react back on the fluid itself, interact with each other, or even collide.

The results summarized above show that the century-old ansatz of scale separation may not be sufficient to describe the relevant properties of real-world turbulence. New theoretical concepts must be developed and tested in experiments, numerical simulations, and theory not only to advance our understanding of turbulence phenomena per se, but also to better address nonideal turbulence realizations at the various levels observed in nature.

Many transport problems (e.g., thermal convection) depend on the cumulative effect and coupling of motions at all scales. The future challenge of turbulence research will have to deal with the factoring of idealized versus nonidealized situations and how these influences impact the physics.

DISCLOSURE STATEMENT

The authors are not aware of any biases that might be perceived as affecting the objectivity of this review.

ACKNOWLEDGMENTS

We are indebted to Jeremie Bec, Roberto Benzi, Luca Biferale, Enrico Calzavarini, Massimo Cencini, Laurent Chevillard, Herman Clercx, Lance Collins, Alessandra Lanotte, Beat Luethi, Emmanuel Lévêque, Detlef Lohse, Nick T. Ouellette, Walter Pauls, Jean-François Pinton, Alain Pumir, Andrea Scagliarini, Peichun Tsai, Zellman Warhaft, Haitao Xu, and Pui-Kuen Yeung for contributions, suggestions, and careful reading of the manuscript during its preparation. An increasing number of data sets, including those on Lagrangian turbulence, are available in a raw, unprocessed format at the International CFD Database (iCFDdatabase) accessible at **http://cfd.cineca.it**. Further information on Lagrangian turbulence is available at the ICTR website (**http://www.ictr.eu/**).

LITERATURE CITED

Arimitsu T, Arimitsu N. 2004. Multifractal analysis of fluid particle accelerations in turbulence. *Phys. D* 193:218–30

Arneodo A, Baudet C, Belin F, Benzi R, Castaing B, et al. 1996. Structure functions in turbulence, in various flow configurations, at Reynolds number between 30 and 5000, using extended self-similarity. *Europhys. Lett.* 34:411–16

Arneodo A, Benzi R, Berg J, Biferale L, Bodenschatz E, et al. 2008. Universal intermittent properties of particle trajectories in highly turbulent flows. *Phys. Rev. Lett.* 100:254504

Auton T, Hunt J, Prud'homme M. 1988. The force exerted on a body in inviscid unsteady nonuniform rotational flow. *J. Fluid Mech.* 197:241–57

Ayyalasomayajula S, Gylfason A, Collins L, Bodenschatz E, Warhaft Z. 2006. Lagrangian measurements of inertial particle accelerations in grid generated wind tunnel turbulence. *Phys. Rev. Lett.* 97:144507
Ayyalasomayajula S, Warhaft Z, Collins LR. 2008. Modeling inertial particle acceleration statistics in isotropic turbulence. *Phys. Fluids.* In press
Babiano A, Cartwright JHE, Piro O, Provenzale A. 2000. Dynamics of a small neutrally buoyant sphere in a fluid and targeting in Hamiltonian systems. *Phys. Rev. Lett.* 84:5764–67
Balachandar S, Maxey MR. 1989. Methods for evaluating fluid velocities in spectral simulations of turbulence. *J. Comput. Phys.* 83:96–125
Balkovsky E, Falkovich G, Fouxon A. 2001. Intermittent distribution of inertial particles in turbulent flows. *Phys. Rev. Lett.* 86:2790–93
Bec J. 2003. Fractal clustering of inertial particles in random flows. *Phys. Fluids* 15:L81–84
Bec J, Biferale L, Boffetta G, Celani A, Cencini M, et al. 2006a. Acceleration statistics of heavy particles in turbulence. *J. Fluid Mech.* 550:349–58
Bec J, Biferale L, Boffetta G, Cencini M, Lanotte A, et al. 2006b. Lyapunov exponents of heavy particles in turbulence. *Phys. Fluids* 18:091702
Bec J, Biferale L, Cencini M, Lanotte A, Musacchio S, Toschi F. 2007. Heavy particle concentration in turbulence at dissipative and inertial scales. *Phys. Rev. Lett.* 98:084502
Bec J, Biferale L, Cencini M, Lanotte AS, Toschi F. 2006c. Effects of vortex filaments on the velocity of tracers and heavy particles in turbulence. *Phys. Fluids* 18:081702
Beck C. 2001. Dynamical foundations of nonextensive statistical mechanics. *Phys. Rev. Lett.* 87:180601
Beck C. 2003. Lagrangian acceleration statistics in turbulent flows. *Europhys. Lett.* 64:151–57
Beck C. 2007. Statistics of three-dimensional Lagrangian turbulence. *Phys. Rev. Lett.* 98:064502
Benzi R, Ciliberto S, Tripiccione R, Baudet C, Massaioli F, Succi S. 1993. Extended self-similarity in turbulent flows. *Phys. Rev. E* 48:R29–32
Benzi R, Paladin G, Parisi G, Vulpiani A. 1984. On the multifractal nature of fully developed turbulence and chaotic systems. *J. Phys. A Math. Gen.* 17:3521–31
Bewley GP, Lathrop DP, Sreenivasan KR. 2006. Superfluid helium: visualization of quantized vortices. *Nature* 441:588
Biferale L, Bodenschatz E, Cencini M, Lanotte AS, Ouellette NT, et al. 2008. Lagrangian structure functions in turbulence: a quantitative comparison between experiment and direct numerical simulation. *Phys. Fluids* 20:065103
Biferale L, Boffetta G, Celani A, Devenish B, Lanotte A, Toschi F. 2004a. Multifractal statistics of Lagrangian velocity and acceleration in turbulence. *Phys. Rev. Lett.* 93:064502
Biferale L, Boffetta G, Celani A, Devenish B, Lanotte A, Toschi F. 2005a. Lagrangian statistics of particle pairs in homogeneous isotropic turbulence. *Phys. Fluids* 17:115101
Biferale L, Boffetta G, Celani A, Devenish BJ, Lanotte A, Toschi F. 2005b. Multiparticle dispersion in fully developed turbulence. *Phys. Fluids* 17:111701
Biferale L, Boffetta G, Celani A, Lanotte A, Toschi F. 2005c. Particle trapping in three-dimensional fully developed turbulence. *Phys. Fluids* 17:021701
Biferale L, Boffetta G, Celani A, Lanotte A, Toschi F. 2006. Lagrangian statistics in fully developed turbulence. *J. Turbul.* 7:N6
Biferale L, Boffetta G, Celani A, Toschi F. 1999. Multi-time, multi-scale correlation functions in turbulence and in turbulent models. *Phys. D* 127:187–97
Biferale L, Daumont I, Lanotte A, Toschi F. 2004b. Theoretical and numerical study of highly anisotropic turbulent flows. *Eur. J. Mech. B Fluids* 23:401–14
Biferale L, Toschi F. 2005. Joint statistics of acceleration and vorticity in fully developed turbulence. *J. Turbul.* 6:N40
Boffetta G, Celani A, Lillo FD, Musacchio S. 2007. The Eulerian description of dilute collisionless suspension. *Europhys. Lett.* 78:14001
Boffetta G, De Lillo F, Musacchio S. 2002. Lagrangian statistics and temporal intermittency in a shell model of turbulence. *Phys. Rev. E* 66:066307
Boffetta G, Mazzino A, Vulpiani A. 2008. Twenty-five years of multifractals in fully developed turbulence: a tribute to Giovanni Paladin. *J. Phys. A* 41:363001

Borgas MS. 1993. The multifractal Lagrangian nature of turbulence. *Philos. Trans. Phys. Sci. Eng.* 342:379–411
Bosse T, Kleiser L, Meiburg E. 2006. Small particles in homogeneous turbulence: settling velocity enhancement by two-way coupling. *Phys. Fluids* 18:027102
Bourgoin M, Ouellette NT, Xu H, Berg J, Bodenschatz E. 2006. The role of pair dispersion in turbulent flow. *Science* 311:835–38
Bou-Zeid E, Meneveau C, Parlange M. 2005. A scale-dependent Lagrangian dynamic model for large eddy simulation of complex turbulent flows. *Phys. Fluids* 17:025105
Braun W, De Lillo F, Eckhardt B. 2006. Geometry of particle paths in turbulent flows. *J. Turbul.* 7:N62
Burton TM, Eaton JK. 2005. Fully resolved simulations of particle-turbulence interaction. *J. Fluid Mech.* 545:67–111
Calzavarini E, Cencini M, Lohse D, Toschi F. 2008a. Quantifying turbulence induced segregation on inertial particles. *Phys. Rev. Lett.* 101:084504
Calzavarini E, Kerscher M, Lohse D, Toschi F. 2008b. Minkowski functionals: characterizing particle and bubble clusters in turbulent flow. *J. Fluid Mech.* 607:13–24
Calzavarini E, van den Berg TH, Toschi F, Lohse D. 2008c. Quantifying microbubble clustering in turbulent flow from single-point measurements. *Phys. Fluids* 20:040702
Castiglione P, Pumir A. 2001. Evolution of triangles in a two-dimensional turbulent flow. *Phys. Rev. E* 64:056303
Cate AT, Derksen JJ, Portela LM, Van den Akker HEA. 2004. Fully resolved simulations of colliding monodisperse spheres in forced isotropic turbulence. *J. Fluid Mech.* 519:233–71
Celani A. 2007. The frontiers of computing in turbulence: challenges and perspectives. *J. Turbul.* 8:N34
Celani A, Vergassola M. 2001. Statistical geometry in scalar turbulence. *Phys. Rev. Lett.* 86:424–27
Cencini M, Bec J, Biferale L, Boffetta G, Celani A, et al. 2006. Dynamics and statistics of heavy particles in turbulent flows. *J. Turbul.* 7:N36
Chen L, Goto S, Vassilicos JC. 2006. Turbulent clustering of stagnation points and inertial particles. *J. Fluid Mech.* 553:143–54
Chertkov M, Pumir A, Shraiman BI. 1999. Lagrangian tetrad dynamics and the phenomenology of turbulence. *Phys. Fluids* 11:2394–410
Chevillard L, Castaing B, Lévêque E, Arneodo A. 2006. Unified multifractal description of velocity increments statistics in turbulence: intermittency and skewness. *Phys. D* 218:77–82
Chevillard L, Meneveau C. 2006. Lagrangian dynamics and statistical geometric structure of turbulence. *Phys. Rev. Lett.* 97:174501
Chevillard L, Roux SG, Levêque E, Mordant N, Pinton JF, Arneodo A. 2003. Lagrangian velocity statistics in turbulent flows: effects of dissipation. *Phys. Rev. Lett.* 91:214502
Chong MS, Perry AE, Cantwell BJ. 1990. A general classification of three-dimensional flow fields. *Phys. Fluids A* 2:765–77
Constantin P. 2001. An Eulerian-Lagrangian approach for incompressible fluids: local theory. *J. Am. Math. Soc.* 14:263–78
Crawford A, Mordant N, Bodenschatz E. 2005. Joint statistics of the Lagrangian acceleration and velocity in fully developed turbulence. *Phys. Rev. Lett.* 94:024501
Crisanti A, Falcioni M, Provenzale A, Tanga P, Vulpiani A. 1992. Dynamics of passively advected impurities in simple two-dimensional flow models. *Phys. Fluids A.* 4:1805–20
Douady S, Couder Y, Brachet ME. 1991. Direct observation of the intermittency of intense vorticity filaments in turbulence. *Phys. Rev. Lett.* 67:983–86
Eaton JK, Fessler JR. 1994. Preferential concentration of particles by turbulence. *Int. J. Multiph. Flow* 20:169–209
Elenbaas T. 2005. *Writing lines in turbulent air using Air Photolysis and Recombination Tracking*. Ph.D. thesis. Tech. Univ. Eindhoven
Falkovich G, Fouxon A, Stepanov MG. 2002. Acceleration of rain initiation by cloud turbulence. *Nature* 419:151–54
Falkovich G, Gawedzki K, Vergassola M. 2001. Particles and fields in fluid turbulence. *Rev. Mod. Phys.* 73:913–75

Falkovich G, Pumir A. 2004. Intermittent distribution of heavy particles in a turbulent flow. *Phys. Fluids* 16:L47–50

Frisch U. 1995. *Turbulence: The Legacy of A.N. Kolmogorov*. Cambridge: Cambridge Univ. Press

Gasteuil Y, Shew WL, Gibert M, Chilla F, Castaing B, Pinton JF. 2007. Lagrangian temperature, velocity, and local heat flux measurement in Rayleigh-Bénard convection. *Phys. Rev. Lett.* 99:234302

Gatignol R. 1983. The Faxen formulae for a rigid particle in an unsteady nonuniform stokes flow. *J. Mec. Theor. Appl.* 1:143–60

Gerashchenko S, Sharp N, Neuscamman S, Warhaft Z. 2008. Lagrangian measurements of inertial particle accelerations in a turbulent boundary layer. *J. Fluid Mech.* In press

Goto S, Vassilicos JC. 2006. Self-similar clustering of inertial particles and zero-acceleration points in fully developed two-dimensional turbulence. *Phys. Fluids* 18:115103

Gotoh T, Fukayama D, Nakano T. 2002. Velocity field statistics in homogeneous steady turbulence obtained using a high-resolution direct numerical simulation. *Phys. Fluids* 14:1065–81

Gotoh T, Kraichnan RH. 2004. Turbulence and Tsallis statistics. *Phys. D* 193:231–44

Guala M, Lüthi B, Liberzon A, Tsinober A, Kinzelbach W. 2005. On the evolution of material lines and vorticity in homogeneous turbulence. *J. Fluid Mech.* 533:339–59

Gulitski G, Kholmyansky M, Kinzelbach W, Luethi B, Tsinober A, Yorish S. 2007a. Velocity and temperature derivatives in high-Reynolds-number turbulent flows in the atmospheric surface layer. Part 1. Facilities, methods and some general results. *J. Fluid Mech.* 589:57–81

Gulitski G, Kholmyansky M, Kinzelbach W, Luethi B, Tsinober A, Yorish S. 2007b. Velocity and temperature derivatives in high-Reynolds-number turbulent flows in the atmospheric surface layer. Part 2. Accelerations and related matters. *J. Fluid Mech.* 589:83–102

Gylfason A, Ayyalasomayajula S, Warhaft Z. 2004. Intermittency, pressure and acceleration statistics from hot-wire measurements in wind-tunnel turbulence. *J. Fluid Mech.* 501:213–29

Hill RJ, Wilczak JM. 1995. Pressure structure functions and spectra for locally isotropic turbulence. *J. Fluid Mech.* 296:247–69

Holzner M, Liberzon A, Nikitin N, Luethi B, Kinzelbach W, Tsinober A. 2008. A Lagrangian investigation of the small-scale features of turbulent entrainment through particle tracking and direct numerical simulation. *J. Fluid Mech.* 598:465–75

Homann H, Dreher J, Grauer R. 2007a. Impact of the floating-point precision and interpolation scheme on the results of DNS of turbulence by pseudospectral codes. *Comput. Phys. Commun.* 177:560–65

Homann H, Grauer R, Busse A, Muller WC. 2007b. Lagrangian statistics of Navier-Stokes and MHD turbulence. *J. Plasma Phys.* 73:821–30

Hoyer K, Holzner M, Lüthi B, Guala M, Liberzon A, Kinzelbach W. 2005. 3D scanning particle tracking velocimetry. *Exp. Fluids* 39:923–34

Ishihara T, Kaneda Y, Yokokawa M, Itakura K, Uno A. 2007. Small-scale statistics in high-resolution direct numerical simulation of turbulence: Reynolds number dependence of one-point velocity gradient statistics. *J. Fluid Mech.* 592:335–66

Kolmogorov AN. 1941. The local structure of turbulence in incompressible viscous fluids for very large Reynolds numbers. *Dokl. Acad. Nauk. SSSR* 30:9–13

Kostinski AB, Shaw RA. 2005. Fluctuations and luck in droplet growth by coalescence. *Bull. Am. Meteorol. Soc.* 86:235–44

Kraichnan RH. 1966. Isotropic turbulence and inertial-range structure. *Phys. Fluids* 9:1728–52

Kurien S, L'vov V, Procaccia I, Sreenivasan K. 2000. Scaling structure of the velocity statistics in atmospheric boundary layers. *Phys. Rev. E* 61:407–21

Lamorgese AG, Pope SB, Yeung PK, Sawford BL. 2007. A conditionally cubic-Gaussian stochastic Lagrangian model for acceleration in isotropic turbulence. *J. Fluid Mech.* 582:423–48

La Porta A, Voth GA, Crawford AM, Alexander J, Bodenschatz E. 2001. Fluid particle accelerations in fully developed turbulence. *Nature* 409:1017–19

La Porta A, Voth GA, Moisy F, Bodenschatz E. 2000. Using cavitation to measure statistics of low-pressure events in large-Reynolds-number turbulence. *Phys. Fluids* 12:1485–96

Lee S, Lee C. 2005. Intermittency of acceleration in isotropic turbulence. *Phys. Rev. E* 71:056310–15

Lehmann B, Nobach H, Tropea C. 2002. Measurement of acceleration using the laser Doppler technique. *Meas. Sci. Technol.* 13:1367–81
Lüthi B, Ott S, Berg J, Mann J. 2007. Lagrangian multi-particle statistics. *J. Turbul.* 8:N45
Lüthi B, Tsinober A, Kinzelbach W. 2005. Lagrangian measurement of vorticity dynamics in turbulent flow. *J. Fluid Mech.* 528:87–118
L'vov VS, Podivilov E, Procaccia I. 1997. Temporal multiscaling in hydrodynamic turbulence. *Phys. Rev. E* 55:7030–35
Maxey M. 1987. The motion of small spherical particles in a cellular flow field. *Phys. Fluids* 30:1915
Maxey MR, Riley JJ. 1983. Equation of motion for a small rigid sphere in a nonuniform flow. *Phys. Fluids* 26:883–89
Mazzitelli IM, Lohse D. 2004. Lagrangian statistics for fluid particles and bubbles in turbulence. *New J. Phys.* 6:203
Mazzitelli IM, Lohse D, Toschi F. 2003a. The effect of microbubbles on developed turbulence. *Phys. Fluids* 15:L5–8
Mazzitelli IM, Lohse D, Toschi F. 2003b. On the relevance of the lift force in bubbly turbulence. *J. Fluid Mech.* 488:283–313
Meneveau C, Lund TS, Cabot WH. 1996. A Lagrangian dynamic subgrid-scale model of turbulence. *J. Fluid Mech. Digit. Arch.* 319:353–85
Miles R, Lempert W, Zhang B. 1991. Turbulent structure measurements by relief flow tagging. *Fluid Dyn. Res.* 8:9–17
Moisy F, Jiménez J. 2004. Geometry and clustering of intense structures in isotropic turbulence. *J. Fluid Mech.* 513:111–33
Monaghan JJ. 1988. An introduction to SPH. *Comput. Phys. Commun.* 48:89–96
Monin AS, Yaglom AM. 1975. *Statistical Fluid Mechanics*. Cambridge, MA: MIT Press
Mordant N, Crawford AM, Bodenschatz E. 2004a. Experimental Lagrangian acceleration probability density function measurement. *Phys. D* 193:245–51
Mordant N, Crawford AM, Bodenschatz E. 2004b. Three-dimensional structure of the Lagrangian acceleration in turbulent flows. *Phys. Rev. Lett.* 93:214501
Mordant N, Delour J, Léveque E, Arnéodo A, Pinton JF. 2002. Long time correlations in Lagrangian dynamics: a key to intermittency in turbulence. *Phys. Rev. Lett.* 89:254502
Mordant N, Lévêque E, Pinton JF. 2004c. Experimental and numerical study of the Lagrangian dynamics of high Reynolds turbulence. *New J. Phys.* 6:116
Mordant N, Metz P, Michel O, Pinton JF. 2001. Measurement of Lagrangian velocity in fully developed turbulence. *Phys. Rev. Lett.* 87:214501
Mydlarski L, Warhaft Z. 1998. Passive scalar statistics in high-Péclet-number grid turbulence. *J. Fluid Mech.* 358:135–75
Nelkin M. 2000. Resource letter TF-1: turbulence in fluids. *Am. J. Phys.* 68:310–18
Ott E. 2002. *Chaos in Dynamical Systems*. Cambridge: Cambridge Univ. Press. 2nd ed.
Ott S, Mann J. 2000. An experimental investigation of the relative diffusion of particle pairs in three-dimensional turbulent flow. *J. Fluid Mech.* 422:207–23
Ouellette NT, Xu H, Bourgoin M, Bodenschatz E. 2006a. An experimental study of turbulent relative dispersion models. *New J. Phys.* 8:109
Ouellette NT, Xu H, Bourgoin M, Bodenschatz E. 2006b. Small-scale anisotropy in Lagrangian turbulence. *New J. Phys.* 8:102
Parisi G, Frisch U. 1985. On the singularity structure of fully developed turbulence. In *Turbulence and Predictability of Geophysical Fluid Dynamics*, ed. M Ghil, R Benzi, G Parisi. Amsterdam: North-Holland
Perrin A, Hu HH. 2006. An explicit finite-difference scheme for simulation of moving particles. *J. Comput. Phys.* 212:166–87
Pope SB. 2000. *Turbulent Flows*. Cambridge: Cambridge Univ. Press
Pope SB. 2004. Ten questions concerning the large-eddy simulation of turbulent flows. *New J. Phys.* 6:35
Pumir A, Shraiman BI, Chertkov M. 2000. Geometry of Lagrangian dispersion in turbulence. *Phys. Rev. Lett.* 85:5324–27

Pumir A, Shraiman B, Chertkov M. 2001. The Lagrangian view of energy transfer in turbulent flow. *Europhys. Lett.* 56:379–85
Qureshi NM, Bourgoin M, Baudet C, Cartellier A, Gagne Y. 2007. Turbulent transport of material particles: an experimental study of finite size effects. *Phys. Rev. Lett.* 99:184502
Reynolds AM. 2003. On the application of nonextensive statistics to Lagrangian turbulence. *Phys. Fluids* 15:L1–4
Riley JJ, Patterson GSJ. 1974. Diffusion experiments with numerically integrated isotropic turbulence. *Phys. Fluids* 17:292–97
Rovelstad AL, Handler RA, Bernard PS. 1994. The effect of interpolation errors on the Lagrangian analysis of simulated turbulent channel flow. *J. Comput. Phys.* 110:190–95
Salazar JPLC, Collins LR. 2009. Two-particle dispersion in isotropic turbulent flows. *Annu. Rev. Fluid Mech.* 41:In press
Salazar JPLC, De Jong J, Cao L, Woodward SH, Meng H, Collins LR. 2008. Experimental and numerical investigation of inertial particle clustering in isotropic turbulence. *J. Fluid Mech.* 600:245–56
Sato Y, Yamamoto K. 1987. Lagrangian measurement of fluid-particle motion in an isotropic turbulent field. *J. Fluid Mech.* 175:183–99
Saw EW, Shaw RA, Ayyalasomayajula S, Chuang PY, Gylfason A. 2008. Inertial clustering of particles in high-Reynolds-number turbulence. *Phys. Rev. Lett.* 100:214501–4
Sawford B. 2001. Turbulent relative dispersion. *Annu. Rev. Fluid Mech.* 33:289–317
Sawford B, Yeung P, Borgas M, Vedula P, La Porta A, et al. 2003. Conditional and unconditional acceleration statistics in turbulence. *Phys. Fluids* 15:3478–89
Sawford BL, Guest FM. 1991. Lagrangian statistical simulation of the turbulent motion of heavy particles. *Bound.-Layer Meteorol.* 54:147–66
Schumacher J. 2007. Sub-Kolmogorov-scale fluctuations in fluid turbulence. *Europhys. Lett.* 80:54001
Shaw RA. 2003. Particle-turbulence interactions in atmospheric clouds. *Annu. Rev. Fluid Mech.* 35:183–227
She ZS, Jackson E, Orszag SA. 1991. Structure and dynamics of homogeneous turbulence: models and simulations. *Proc. Math. Phys. Sci.* 434:101–24
Shew WL, Gasteuil Y, Gibert M, Metz P, Pinton JF. 2007. Instrumented tracer for Lagrangian measurements in Rayleigh-Bénard convection. *Rev. Sci. Instrum.* 78:065105
Shlien DJ, Corrsin S. 1974. A measurement of Lagrangian velocity autocorrelation in approximately isotropic turbulence. *J. Fluid Mech.* 62:255–71
Shraiman BI, Siggia ED. 2000. Scalar turbulence. *Nature* 405:639–46
Siggia ED. 1981. Numerical study of small-scale intermittency in three-dimensional turbulence. *J. Fluid Mech.* 107:375–406
Snyder WH, Lumley JL. 1971. Some measurements of particle velocity autocorrelation functions in a turbulent flow. *J. Fluid Mech.* 48:41–71
Squires KD, Eaton JK. 1991. Preferential concentration of particles by turbulence. *Phys. Fluids A* 3:1169
Sundaram S, Collins LR. 1999. A numerical study of the modulation of isotropic turbulence by suspended particles. *J. Fluid Mech.* 379:105–43
Tabeling P, Zocchi G, Belin F, Maurer J, Willaime H. 1996. Probability density functions, skewness and flatness in large Reynolds number turbulence. *Phys. Rev. E* 53:1613
Taylor GI. 1921. Diffusion by continuous movements. *Proc. Lond. Math. Soc.* 20:196–211
Tennekes H, Lumley JL. 1972. *A First Course in Turbulence*. Cambridge, MA: MIT Press
Toschi F, Bec J, Biferale L, Boffetta G, Celani A, et al. 2008. Acceleration statistics of inertial particles from high resolution DNS turbulence. In *IUTAM Sympos. Comput. Phys. New Perspect. Turbul.*, ed. Y Kaneda, pp. 73–78. Dordrecht: Springer-Verlag
Toschi F, Biferale L, Boffetta G, Celani A, Devenish BJ, Lanotte A. 2005. Acceleration and vortex filaments in turbulence. *J. Turbul.* 6:N15
Unverdi SO, Tryggvason G. 1992. A front-tracking method for viscous, incompressible, multi-fluid flows. *J. Comput. Phys.* 100:25–37
van Aartrijk M, Clercx HJH. 2008. Preferential concentration of heavy particles in stably stratified turbulence. *Phys. Rev. Lett.* 100:254501

van Aartrijk M, Clercx HJH, Winters KB. 2008. Single-particle, particle-pair, and multiparticle dispersion of fluid particles in forced stably stratified turbulence. *Phys. Fluids* 20:025104–16

Van Nierop EA, Luther S, Bluemink JJ, Magnaudet J, Prosperetti A, Lohse D. 2007. Drag and lift forces on bubbles in a rotating flow. *J. Fluid Mech.* 571:439–54

Vedula P, Yeung PK. 1999. Similarity scaling of acceleration and pressure statistics in numerical simulations of isotropic turbulence. *Phys. Fluids* 11:1208–20

Vincent A, Meneguzzi M. 1991. The spatial structure and statistical properties of homogeneous turbulence. *J. Fluid Mech.* 225:1–20

Virant M, Dracos T. 1997. 3D PTV and its application on Lagrangian motion. *Meas. Sci. Technol.* 8:1539–52

Volk R, Calzavarini E, Verhille G, Lohse D, Mordant N, et al. 2008a. Acceleration of heavy and light particles in turbulence: comparison between experiments and direct numerical simulations. *Phys. D* 237:2084–89

Volk R, Mordant N, Verhille G, Pinton JF. 2008b. Laser Doppler measurement of inertial particle and bubble accelerations in turbulence. *Europhys. Lett.* 81:34002

Voth GA, La Porta A, Crawford AM, Alexander J, Bodenschatz E. 2002. Measurement of particle accelerations in fully developed turbulence. *J. Fluid Mech.* 469:121–60

Voth GA, La Porta A, Crawford AM, Bodenschatz E, Ward C, Alexander J. 2001. A silicon strip detector system for high resolution particle tracking in turbulence. *Rev. Sci. Instrum.* 72:4348–53

Voth GA, Satyanarayan K, Bodenschatz E. 1998. Lagrangian acceleration measurements at large Reynolds numbers. *Phys. Fluids* 10:2268–80

Warhaft Z. 2008. Laboratory studies of droplets in turbulence: towards understanding the formation of clouds. *Fluid Dyn. Res.* In press

Weil JC, Sykes RI, Venkatram A. 1992. Evaluating air-quality models: review and outlook. *J. Appl. Meteorol.* 31:1121–45

Xu A, Succi S, Boghosian BM. 2006a. Lattice BBGKY scheme for two-phase flows: one-dimensional case. *Math. Comput. Simul.* 72:249–52

Xu H, Ouellette NT, Bodenschatz E. 2006b. Multifractal dimension of Lagrangian turbulence. *Phys. Rev. Lett.* 96:114503

Xu H, Ouellette NT, Bodenschatz E. 2007a. Curvature of Lagrangian trajectories in turbulence. *Phys. Rev. Lett.* 98:050201

Xu H, Ouellette NT, Bodenschatz E. 2007b. Multi-particle statistics: lines, shapes, and volumes in high Reynolds number turbulence. *Proc. 5th Int. Conf. Nonlinear Mech.*, ed. W-Z Chien, pp. 1155–61. Shanghai: Shanghai Univ. Press

Xu H, Ouellette NT, Bodenschatz E. 2008. Evolution of geometric structures in intense turbulence. *New J. Phys.* 10:013012

Yang TS, Shy SS. 2005. Two-way interaction between solid particles and air turbulence: particle settling rate and turbulence modification measurements. *J. Fluid Mech.* 526:171–216

Yeung PK. 2002. Lagrangian investigations of turbulence. *Annu. Rev. Fluid Mech.* 34:115–42

Yeung PK, Pope SB. 1988. An algorithm for tracking fluid particles in numerical simulations of homogeneous turbulence. *J. Comput. Phys.* 79:373–416

Yeung PK, Pope SB. 1989. Lagrangian statistics from direct numerical simulations of isotropic turbulence. *J. Fluid Mech.* 207:531–86

Yeung PK, Pope SB, Sawford BL. 2006. Reynolds number dependence of Lagrangian statistics in large numerical simulations of isotropic turbulence. *J. Turbul.* 7:N58

Zeff BW, Lanterman DD, McAllister R, Roy R, Kostelich EJ, Lathrop DP. 2003. Measuring intense rotation and dissipation in turbulent flows. *Nature* 421:146–49

Zhang Z, Prosperetti A. 2005. A second-order method for three-dimensional particle simulation. *J. Comput. Phys.* 210:292–324

Zybin K, Sirota V, Ilyin A, Gurevich A. 2008. Lagrangian statistical theory of fully developed hydrodynamical turbulence. *Phys. Rev. Lett.* 100:174504

Annual Review of
Fluid Mechanics

Volume 41, 2009

Contents

Indexes

Errata

An online log of corrections to *Annual Review of Fluid Mechanics* articles may be found at http://fluid.annualreviews.org/errata.shtml